AD NUMBER

ADB115170

LIMITATION CHANGES

TO:

Approved for public release; distribution is unlimited.

FROM:

Distribution authorized to U.S. Gov't. agencies only; Critical Technology; 03 MAR 1987. Other requests shall be referred to Air Force Global Weather Center, Offutt AFB, NE 68113. This document contains export-controlled technical data.

AUTHORITY

USAF ETAC/DOL ltr, 9 Feb 1995

AD NUMBER

B115170

NEW LIMITATION CHANGE

TO Approved for Public Release;
Distribution Unlimited.
** Stmt: A
** Code: 1

FROM

N/A

AUTHORITY

USAFETAC/DOL-19950209

AFGWC/TN - 87/001

AFGWC CLOUD FORECAST MODELS

EDITED BY

MAJOR TIMOTHY D. CRUM

APRIL 1987

UNITED STATES AIR FORCE
AIR WEATHER SERVICE (MAC)
AIR FORCE GLOBAL WEATHER CENTRAL
OFFUTT AFB NE 68113-5000

REVIEW AND APPROVAL STATEMENT

AFGWC/TN-87/001, AFGWC Cloud Forecast Models, April 1987, has been reviewed and is approved for publication.

JOHN W. OLIVER, Colonel, USAF
Chief, Operations Division

FOR THE COMMANDER

KIM A. KARST, Colonel, USAF
Vice Commander

REPORT DOCUMENTATION PAGE

1a. Report Security Classification: UNCLASSIFIED.

3. Distribution/Availability of Report: Distribution authorized to U.S. Government agencies only, to protect information otherwise releasable only IAW DOD Instruction 7930.2, 1 April 1987. Other requests for this document shall be referred to HQ AFGWC/CV.

4. Performing Organization Report Number: AFGWC/TN-87/001.

6a. Name of Performing Organization: Air Force Global Weather Central.

6b. Office Symbol: AFGWC/SDDC.

6c. Address: Offutt AFB, NE 68113-5000.

11. Title: AFGWC Cloud Forecast Models.

13a. Type of Report: Technical Note.

14. Date of Report: April 1987.

15. Page Count: 76

17. COSATI Codes: Field--04, Group--02.

18. Subject Terms: *CLOUD FORECASTING, meteorology, cloud analysis, trajectories.

19. Abstract: AFGWC has three cloud forecast models: Five-Layer (5LAYER), High Resolution Cloud Prognosis (HRCP), and Tropical Cloud Forecasting Model (TRONEW). These models satisfy a wide range of requirements and have been in operation since the early 1970s. The 5LAYER model makes extra-tropical forecasts for periods up to 48 hours. Forecasts of layer and total cloud, cloud type, layer temperatures, and icing and weather conditions are made. The 5LAYER model uses a quasi-Lagrangian approach to make these forecasts. The trajectories needed for these forecasts are computed from the AWS Global Spectral Model (GSM) derived wind forecasts. The 5LAYER moisture is initialized from the Real-Time Nephanalysis Model (RTNEPH) layer cloud-amount and the Multi-layer Analysis Model (MULTAN) layer dew-point depression. The 5LAYER temperatures are initialized from the High Resolution Analysis System (HIRAS) and GSM derived temperatures. The High Resolution Cloud Prognosis (HRCP) model combines RTNEPH analyzed cloud input with 5LAYER trajectories to produce high resolution (25 nm), short-range (out to 9 hour) cloud forecasts. The TRONEW model uses the analyzed RTNEPH cloud to make 24 hour persistence cloud forecasts for the tropics.

20. Distribution/Availability of Abstract: Same as report.

21. Abstract Security Classification: UNCLASSIFIED.

22a. Name of Responsible Individual: TIMOTHY D. CRUM.

22b. Telephone: 402-294-5503.

22c. Office Symbol: AFGWC/SDDC

PREFACE

This Technical Note (TN) describes the automated moisture and temperature forecast model that currently exists at the Air Force Global Weather Central (AFGWC). The AFGWC uses the forecasts from this model to provide environmental support to the USAF, the U.S. Army, and other DOD agencies. This technical note provides detailed information on the scientific and computational methods used by the model to satisfy military requirements. This informaton will be of particular interest to personnel in military and non-military units associated with DOD activities who use AFGWC cloud and temperature forecasts in operational or developmental work.

We are indebted to the many people who have developed and maintained the "cloud models" over the past ten years. The many notes, letters, studies, and reports which they prepared made this TN possible. Special thanks go to Major Arnold L. Friend and Dr. Kenneth E. Mitchell.

TABLE OF CONTENTS

LIST OF FIGURES

LIST OF TABLES

1. INTRODUCTION

1.1 General Motivation

The need for cloud forecasting models is based upon requirements of the Department of Defense. Clouds, because of their restriction to visibility, severely hamper Air Force and Army decision-makers who must operate in the air and ground environment. The cloud models at AFGWC exist in order to provide input to these decision-makers. They must know whether or not a target can be acquired visually or through cloud or moisture-sensitive guidance systems. The types of targets range from the end of a runway for landing aircraft to battlefield conditions for weapon delivery. Because of these requirements, the need for cloud forecasting exists. The AFGWC cloud models, described in the following sections, are designed to support that need.

1.2 Philosophy

The Five-Layer (5LAYER) model is an automated, synoptic scale, cloud fore casting program. Its primary purpose is to produce cloud forecasts over two hemispheric domains. Figures 1 and 2 show the forecast domain in the Northern Hemisphere (NH) and Southern Hemisphere (SH) respectively. Temperatures and moisture are forecast and combined to produce other forecast parameters such as icing and precipitation type. In this or any model, the user needs to understand the characteristics or properties of the model. With this understanding, the user will be able to anticipate model strengths and weaknesses in order to optimize the application to operational problems.

1.3 History

Automated cloud forecasting at AFGWC began in the late 1960s with the introduction of a trajectory model having a grid resolution of approximately 200 nm over a hemispheric domain.

Later, the basic cloud and temperature forecasts were combined into other forecast elements such as icing and precipitation amount. In the early 1970s, the forerunner of the current 5LAYER model was developed with a relocatable grid of 100 nm resolution.

Also in the early 1970s, a high resolution, limited area, short range forecast capability was appended to the basic model to take advantage of the Three-Dimensional Nephanalysis Model (3DNEPH) (Fye, 1978). The 3DNEPH was succeeded in August 1983 by the Real-Time Nephanalysis (RTNEPH) Model. An improved mathematical technique for calculating the trajectories was adopted during the mid 1970s. About the same time, the 100 nm grid resolution was applied over the entire hemispheric domain thereby eliminating the need for a relocatable grid.

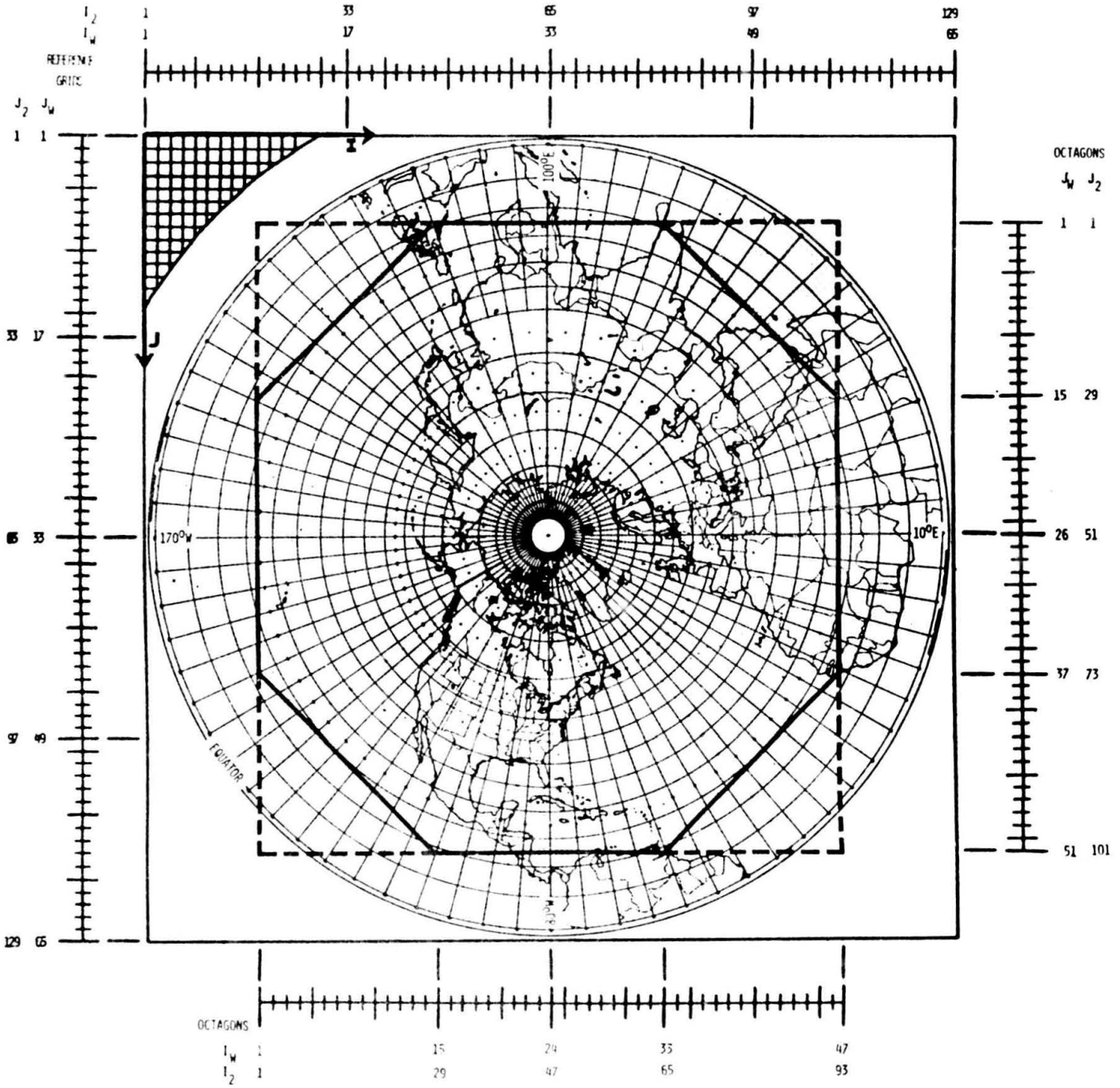

Fig. 1. The Whole-mesh and Half-mesh Octagons for the Northern Hemisphere. Tha domain of the Reference Grids (solid outer border) is also plotted. The indices (I_W, J_W) and (I_2, J_2) designate the coordinates for the whole-mesh and half mesh versions, respectively, with respect to the Octagons and the Reference Grids. The dashed lines indicate that data on the Octagons are actually stored in a rectangular database. The whole-mesh grid spacing is displayed in the upper-left corner. From Hoke et al. (1985).

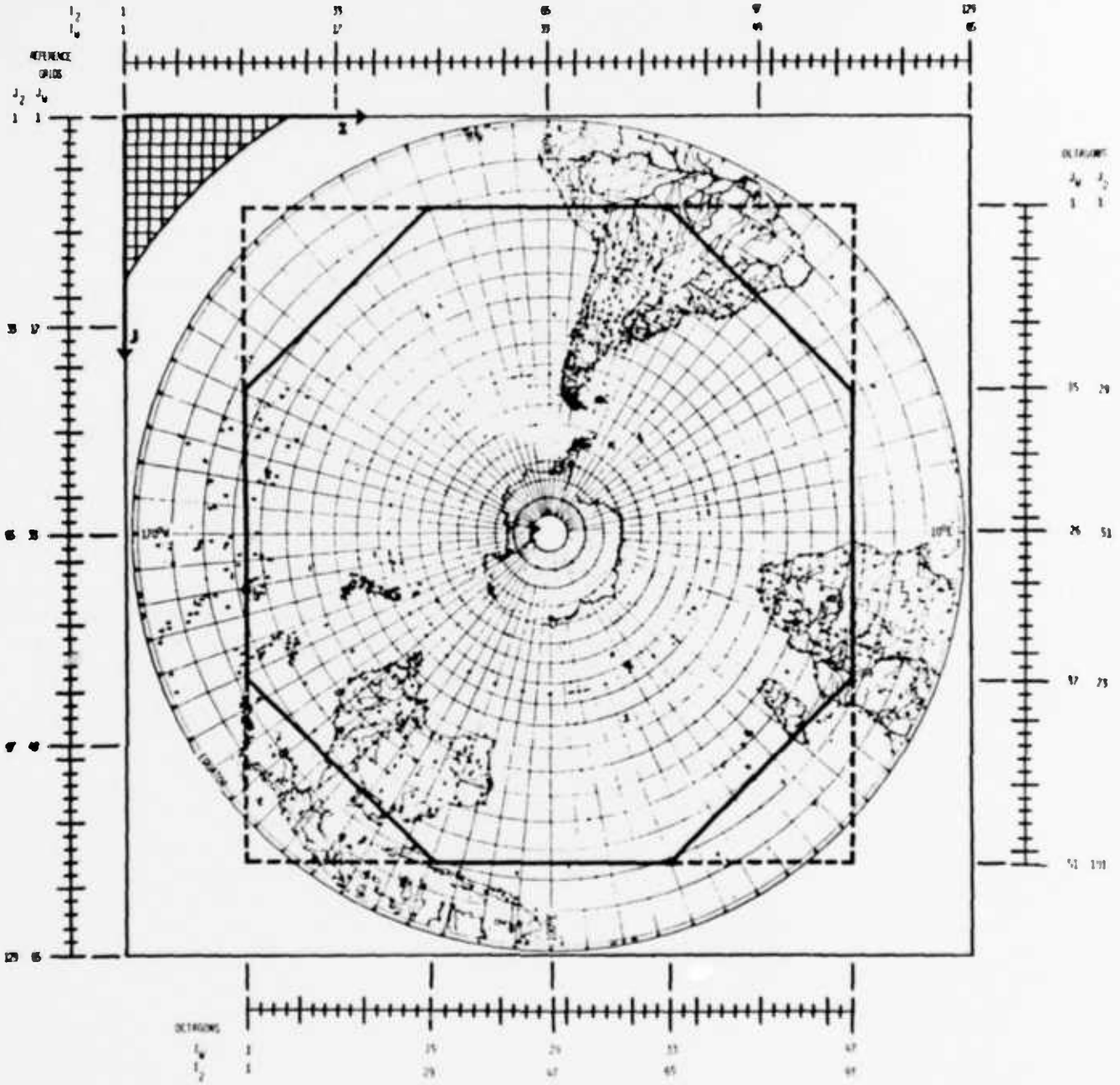

Fig. 2. Same as Fig. 1 except for the Southern Hemisphere.

In 1986, a new initialization module was implemented. This allowed the 5LAYER to be initialized directly from the RTNEPH database. Another major change was the ability of 5LAYER to use its forecast to initialize the moisture field if the analysis data was older than a specified threshold. This threshold is adjustable and presently is set at 4 hours.

1.4 Current Specifications

1.4.1 Forecast Elements

The 5LAYER model forecasts cloud and temperature in three-hour increments out to 48 hours in the NH and 24 hours in the SH. The choice of the three-hour time step is based on convenience rather than necessity. Wind components obtained from the Air Weather Service Global Spectral Model (AWS GSM)(Stobie, 1986), 40 wave and 12 level, are available in three-hour increments; therefore, trajectories are computed to represent parcel movement over that same time increment. In this approach, the length of the time step is unrelated to any numerical stability criteria because the Lagrangian advection scheme of 5LAYER does not explicitly solve finite difference approximations to differential equations.

Temperature forecasts in combination with cloud forecasts can produce additional meteorological elements. Air Force and Army decision-makers are not only concerned with clouds but also with any meteorological element that effects the accomplishment of their mission. Two important elements are precipitation and icing. Conditions that produce aircraft icing must be anticipated by the operational planner. The 5LAYER model uses several methods to produce forecasts of precipitation amount, precipitation type, and icing. Dew point depressions, static stability, and cloud types are forecast to determine these elements.

The discontinuous nature of cloud coverage suggests the need to forecast clouds on a small resolution grid system. However, constraints such as computer capabilities and the need to meet operational time requirements cause the spatial resolution to be less than ideal. The 5LAYER model forecasts for five layers in the vertical and on grid points separated by 100 nm. Even though the horizontal grid spacing is approximately equal to the smallest grid spacing of many operational dynamic models, this spacing causes considerable dilution of the available information. Meteorological satellites routinely resolve cloud elements to one-third of a mile. Averaging or compacting this information to a grid resolution of 100 nm causes smoothing of the data. The problem of data compaction will be discussed later. Users of cloud model forecasts should constantly remind themselves that cloud forecasts represent average cloud conditions over a large volume. This same volume is the "parcel" of air that is referred to throughout this memo.

1.4.2 Forecast Mechanism

Generally, 5LAYER uses a quasi-Lagrangian advection scheme to determine the advected elements. A pure Lagrangian scheme follows a parcel throughout the forecast period. 5LAYER follows the parcel in three-hour increments until the end of the forecast period. A characteristic of this scheme is that the trajectory remains fixed at one end while the other end specifies the source of the parcel. This upstream trajectory requires a gridded analysis to provide values of the element at the source point. The value of the element is determined by interpolation to the source point and modified as it traverses the trajectory path. Since all trajectories terminate at a grid point, a gridded forecast field results. This procedure is repeated with each forecast field serving as the initial field for subsequent forecast increments until the desired forecast length is reached.

The motivation to use this type of forecast scheme lies in the characteristically discontinuous nature of clouds. This discontinuous nature is not easily adaptable to conventional advection schemes which require a smooth, continuous variation of the advected element. Finite difference approximations to differential equations perform best when gradients of the element can be accurately determined. The quasi-Lagrangian approach is an acceptable alternative since gradients of clouds are not resolvable by current numerical models.

1.5 Overview

The remaining sections of this technical note describe specific features of the cloud forecasting models at AFGWC. Section 2 details the initialization procedures of the model for both moisture and temperature. Section 3 discusses the computation of trajectories used to advect the moisture and temperature. Section 4 describes how other physical processes are combined with the advection calculation to obtain the moisture and temperature forecasts. The section then goes on to explain how several additional quantities of meteorological interest are derived from the moisture and temperature forecasts. Section 5 describes the procedures used to obtain a limited area cloud forecast of up to 9 hours at 25 nm resolution. Section 6 discusses the procedures used to forecast clouds in the tropics. In Section 7 verification of the model is reviewed. Several appendices are included to give explicit details of some of the more complex mathematical formulations and the data used for the moisture to cloud amount conversions.

2. INITIALIZATION

2.1 General Characteristics

To produce a numerical forecast, one must first construct analysis fields of the meteorological elements to be forecast. Two such elements of major interest at AFGWC are temperature and moisture. Because of its world-wide mission, AFGWC must forecast these elements on a global basis. To support this requirement, automated, hemispheric, upper-air analysis models produce temperature and dew-point depression analyses. In addition, an automated cloud analysis model supplies initial cloud fields by merging visual and infrared (IR) satellite data with conventional meteorological data. The relationship between analysis and forecast fields requires detailed discussion of cloud and temperature initialization to gain a better understanding of not only the initialization procedures, but also the quality and verification of forecast variables. A conceptual flow chart, Figure 3, summarizes the initialization procedures that will be discussed in the following sections.

2.1.1 Motivation

The quality of a forecast is no greater than the quality of the analysis upon which it is based. For this reason, the initialization of the cloud forecast models is designed to be as consistent and accurate as possible. The input for the cloud forecast models comes from the RTNEPH. The automated RTNEPH analyses contain information on the amount of cloud present, its base and top for up to four cloud layers. This information is based on satellite analyses and conventional meteorological data (surface observations, radiosondes, and aircraft reports). Many factors limit the consistency and accuracy of the initialization of the moisture and temperature variables. These include the grid resolution of the model, the timeliness of the observation, and our understanding of the physics of the atmosphere as related to clouds and moisture.

The grid resolution affects the initialization of moisture because of data compaction. "Compaction" refers to the process of averaging data at one resolution to yield data at a coarser resolution. Very high resolution satellite data is compacted to 25 nm resolution by the RTNEPH and then further compacted to 100 nm to initialize the forecast model. Each reduction in resolution tends to decrease the accuracy of the analysis because the averaging process decreases the sharp distinction between moist and dry areas. Consistency between the analysis of moisture by the RTNEPH and the initialization fields of the forecast model is difficult because the analysis is predominantly based on total cloud data from meteorological satellites while the initialization of the forecast models must be on their distinct pressure surfaces.

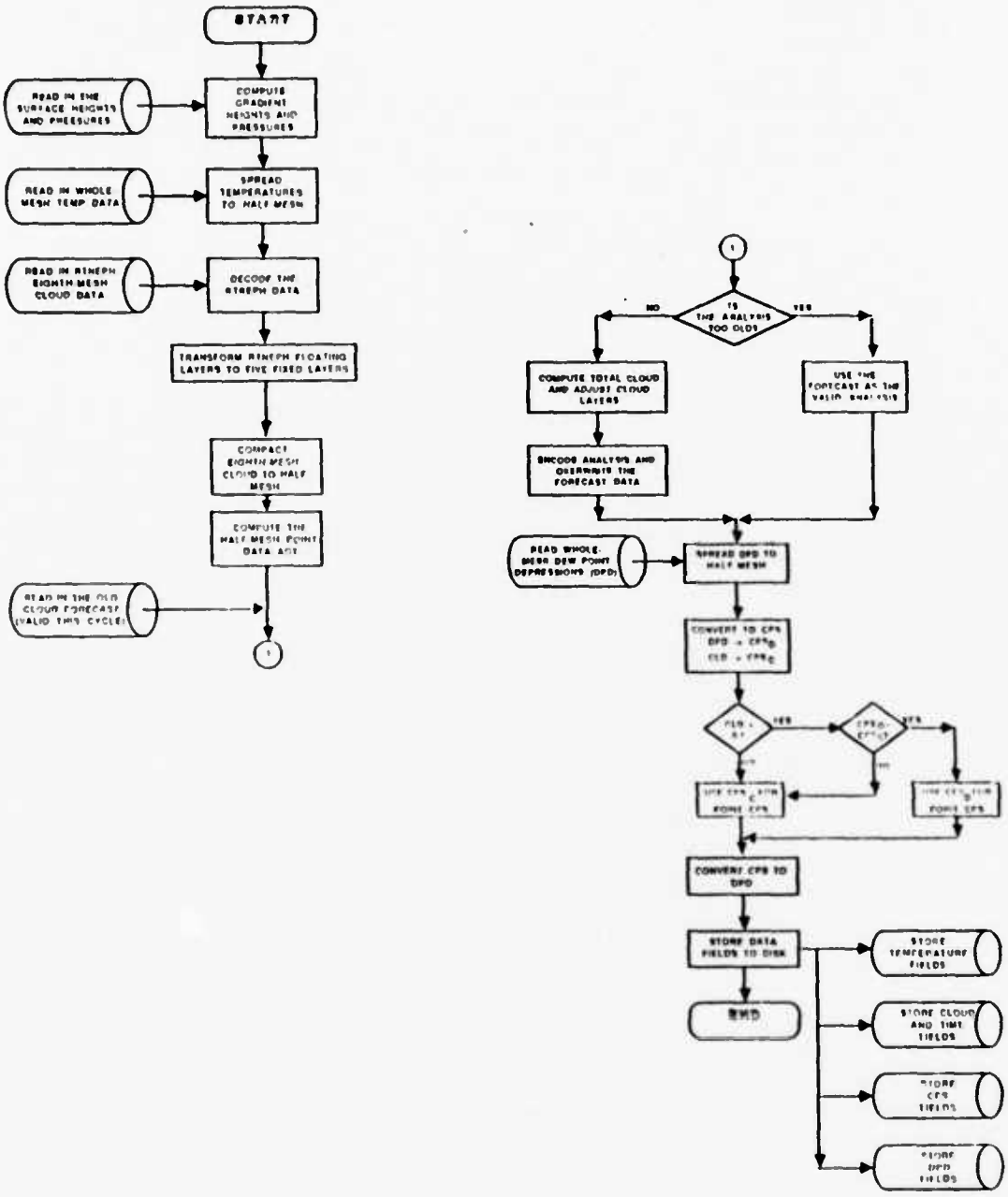

Fig. 3. 5LAYER intialization flow chart.

Since the satellite data used in the RTNEPH is from polar orbiting satellites and the 5LAYER grid covers the extratropical regions of the Northern and Southern hemispheres, the data used to analyze the cloud field can be 8 or more hours old. Instead of using data this old, the model will initialize from cloud forecasts valid at the current cycle time. Even with forecast data, however, fast-moving cloud systems create discontinuities near the edges of overlapping cloud coverage. The discontinuities, in turn, cause inconsistencies in the initialization.

In order to convert from the cloud elements sensed by the satellites to the moisture used as the forecast element, empirical relations have been developed. While these relations have proven to be usable, they still fall short of the accuracy which would be obtained by a specific physical relationship.

The initialization of temperature has the inverse problem of grid resolution since the analyzed temperatures are based upon whole-mesh (200 nm) temperatures which are derived from the High Resolution Analysis System (HIRAS) which is based on a resolution of 2.5 degrees of latitude. The initial temperature values are obtained by interpolating to the 100 nm resolution of the cloud model.

2.1.2 Requirements

The sole purpose of the initialization is to provide an accurate and consistent set of moisture and temperature values with which to start the forecast at each model grid point. As such, the moisture values on the various model surfaces must be consistent enough to be recombined into a total amount that is representative of the total cloud at that grid resolution. Temperature must also satisfy certain conditions. Specifically, the lapse rate must be constrained to avoid superadiabatic conditions. Additionally, model surfaces which intersect the terrain, which can often be at 850 mbs, must have the below ground grid points identified.

2.2 Cloud Initialization

At AFGWC, initial cloud fields are constructed using the Real-Time Nephanalysis Model (RTNEPH). This model combines satellite data, rawinsonde data, conventional surface observations, and aircraft reports to provide up to four layers of cloud information (in percent cloudiness) on a grid spacing of approximately 25 nm. However, because of several operational considerations, this highly detailed information must be compacted to a coarser grid spacing. The AFGWC grid system for cloud and temperature initialization has a horizontal spacing of approximately 100 nm and a vertical resolution of five layers.

2.2.1 Data Compaction.

The AFGWC 200 nm grid, subsequently identified as whole-mesh, is a subset of the RTNEPH horizontal grid. The major difference between these two grid systems is that the RTNEPH grid has points every 25 nm and is referred to as eighth-mesh. The more detailed resolution consists of 262,144 (4096 x 64) horizontal points per hemisphere. At each of these points the RTNEPH analyzes up to four layers of cloud information. At eighth-mesh on a global scale, the 5LAYER model would need to initialize 2,621,440 (262,144 grid points per hemisphere x 2 hemispheres x 5 levels) grid points. The currently available computer hardware, coupled with the time constraints at AFGWC, make it impossible for a prediction model to treat each of these points.

The vertical structure of the RTNEPH grid consists of four floating cloud layers at each point. At any particular point, some or all of the layers may be cloud free. For each layer, the cloud top, bottom, amount, and type are given. The layers are sorted based on cloud tops, from highest to lowest. Total cloud (in percent) is also given for each point, as is a time flag. For 5LAYER to use the RTNEPH data, it must be spread to 5 vertical layers and compacted to a half-mesh horizontal grid.

The RTNEPH data are compacted to reduce the volume of data, while retaining most of the larger-scale information. For example, to construct a value at a half-mesh (100 nm) grid point, the data of the 25 RTNEPH grid points (in the eighth-mesh grid weighting system) that surround this point is used. This data compaction of eighth-mesh points is weighted so that each eighth-mesh grid point influences the final compacted product equally. The scheme in Figure 4 is applicable for all half-mesh grid points that are internal to the grid borders. For those half-mesh points coincident with the grid border the weighting scheme is changed so that the number of eighth-mesh points considered in the half-mesh is correspondingly reduced.

To spread the clouds vertically, the top and base of each layer is checked in turn to see which 5LAYER fixed layers they overlap. The RTNEPH layer amount is inserted into the overlapped 5LAYER layers (unless the receiving layer already has a larger amount in it). The process is repeated for each RTNEPH layer that has cloud in it. Empty layers are skipped.

The vertically spread data is then multiplied by a weighting factor and added to the adjacent half-mesh points. It can be added to up to four points, depending on its position relative to those points. The weighting factor is also added to a weight holding array. The factor is chosen so that no matter how many half-mesh points an eighth-mesh point adds into, its overall contribution is the same. This data composition of eighth-mesh points is weighted so that each eighth-mesh grid point influences the final compacted product equally.

After the weighted eighth-mesh data is added to the half-mesh octagon, the half-mesh values are divided by the respective sum of weights. The resulting point layer cloud amounts are adjusted so the point total cloud is within 2% of the weighted average RTNEPH total cloud at the point.

HORIZONTAL COMPACTION

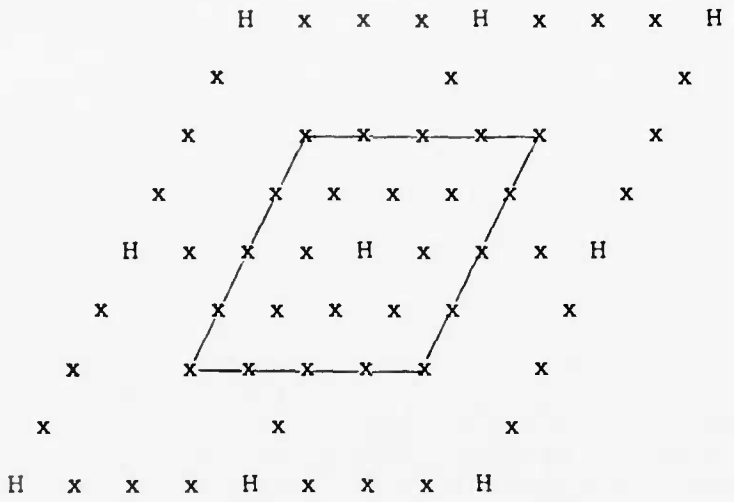

WEIGHTS ASSIGNED

INTERIOR	1.ØØ
SIDE	Ø.5Ø
CORNER	Ø.25

Fig. 4. Weights assigned to eighth-mesh (x) grid point values while compacting to half-mesh (H). The locations (interior, side, corner) are relative to the five-by-five box of eighth-mesh grid points.

2.2.2 Total Cloud Computation

The layered cloud initialization described above is necessary to produce forecasts of layered clouds. Although total cloud is not a direct forecast parameter, it is inferred for verification purposes and some applications. The verification relationship between cloud forecasts and cloud analysis must be made via total cloud because observations of layered cloud are not frequent or detailed enough to satisfy verification requirements. Thus, a precise methodology is required to establish the relationship between layered and total cloud. This methodology must produce a total cloud on the half-mesh grid which closely matches the total cloud amount obtained by horizontal compaction of the RTNEPH total cloud. The total cloud values of the RTNEPH influence the layered cloud initial values of the forecast model and provide verification of previous forecasts.

The total cloud at a point is computed from the statistical union of layer cloud amounts, maximum layer amount and average separation of the cloud layers. Since layer cloud may be separated by thousands of meters, an estimate of how well these layers are correlated is needed.

For example, assume each of five cloud layers contain 50 percent cloud. If the layers are perfectly correlated ($r = 1$), the total cloud amount equals 50 percent, the maximum layer amount. If the layers are independent ($r = 0$), the total cloud amount is about 97 percent, the statistical union of the individual layers.

The actual layer correlation is somewhere between zero and one, so the total cloud in the above example would really be between 50 and 97 percent. The problem is how to estimate this correlation. A conceptual illustration of the vertical cloud stacking problem is given in Figure 5.

A factor, based on layer separation, is used to estimate the layer correlation. The basic assumption is that layers separated by the depth of the troposphere (assumed to be 11000 meters) are uncorrelated ($r = 0$), while those layers immediately adjacent to each other are perfectly correlated ($r = 1$). Intermediately separated layers have correlations which are assumed to vary linearly with mean layer separation:

$$\text{Correlation} = 1 - (\text{Height}_{\text{layer 1}} - \text{Height}_{\text{layer 2}}) / 11000 \qquad (1)$$

For more than two cloud layers, the average of all possible pair-wise separations of the cloud layers is divided by 11000 and then subtracted from one to estimate the correlation.

The final algorithm used to obtain the total cloud is:

(1) Determine the maximum layer cloud amount. This is equal to the minimum total cloud.

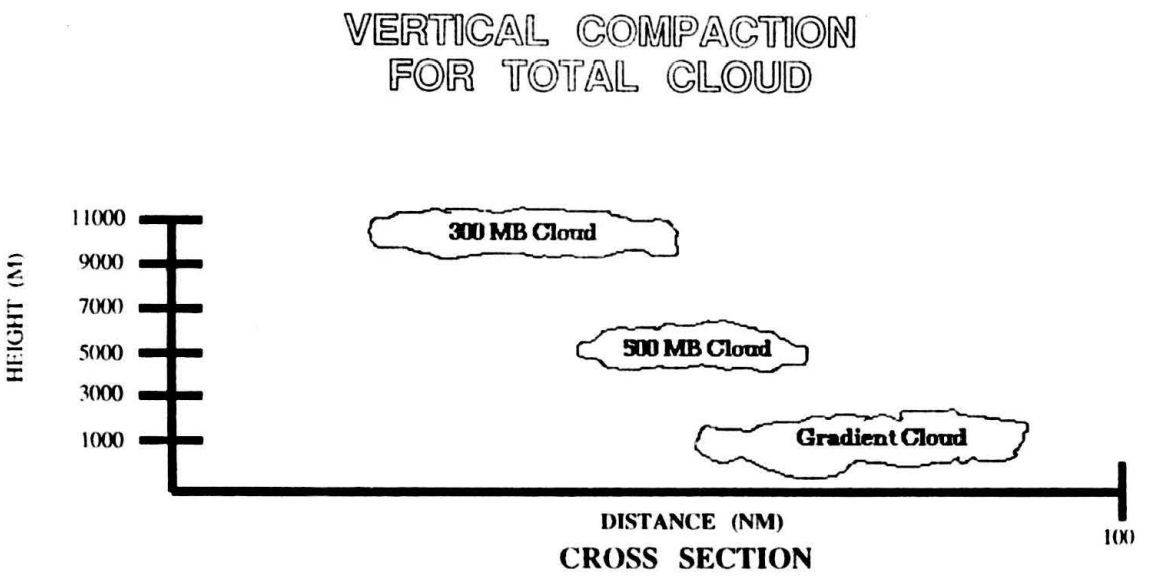

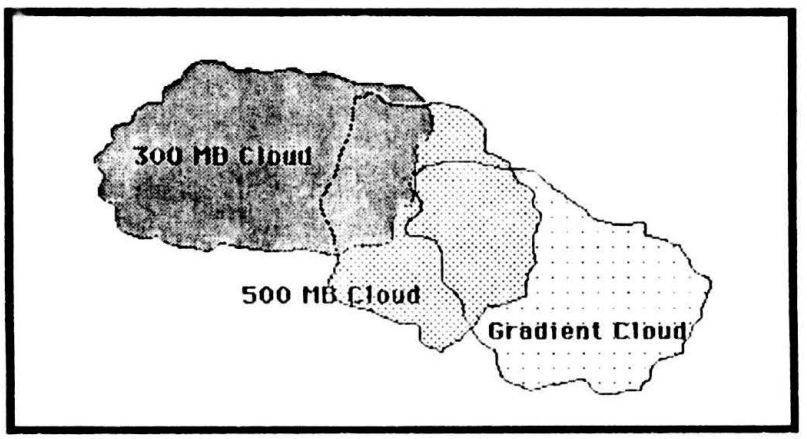

Fig. 5. Side and top view of vertical cloud stacking problem.

(ii) Calculate the statistical union of the layer cloud amounts. This is equal to the maximum total cloud.

(iii) Calculate the mean separation of the cloudy layers, divide by 11000, and subtract from 1. This estimates the correlation.

NOTE: If there are n layers, there are n*(n-1)/2 possible unique pairwise layer separations which need to be averaged to obtain the mean separation.

(iv) Use results from (i) - (iii) to estimate the total cloud:

$$\text{Total} = \text{Min Total} + (\text{Max Total} - \text{Min Total}) * \text{Correlation} \qquad (2)$$

This computed total is then used to adjust the layers (Figure 6) to make them match reality (assumed to be the RTNEPH derived cloud total). The adjustment factor is the RTNEPH total divided by the computed total. If the adjustment factor is greater than 1.02 or less than .98, all the layers are multiplied by the adjustment factor to increase or decrease the layer totals. Then the computed total cloud is recalculated (as above) and the adjustment repeated. The layers will be adjusted up to three times, or until the adjustment factor is in the range .98 - 1.02. In either case, the total cloud used to initialize the 5LAYER database is the RTNEPH total cloud.

2.2.3 Moisture Determination.

2.2.3.1. Moisture in Cloudy Areas.

Condensation pressure spread (CPS) is the moisture parameter used by 5LAYER to forecast cloud amount. CPS is the difference (in millibars) between the pressure of an air parcel and the pressure at which condensation takes place if the parcel is lifted dry adiabatically. Written mathematically,

$$CPS = P - P_s \qquad (3)$$

where P is the pressure of the parcel and P_s is the saturation pressure. See Appendix A for the derivation of equation (3). To calculate CPS at a fixed pressure level, P, only P_s must be specified. An approximate, simplified relationship between CPS in mb and dew-point depression (DPD) in K, can be established as:

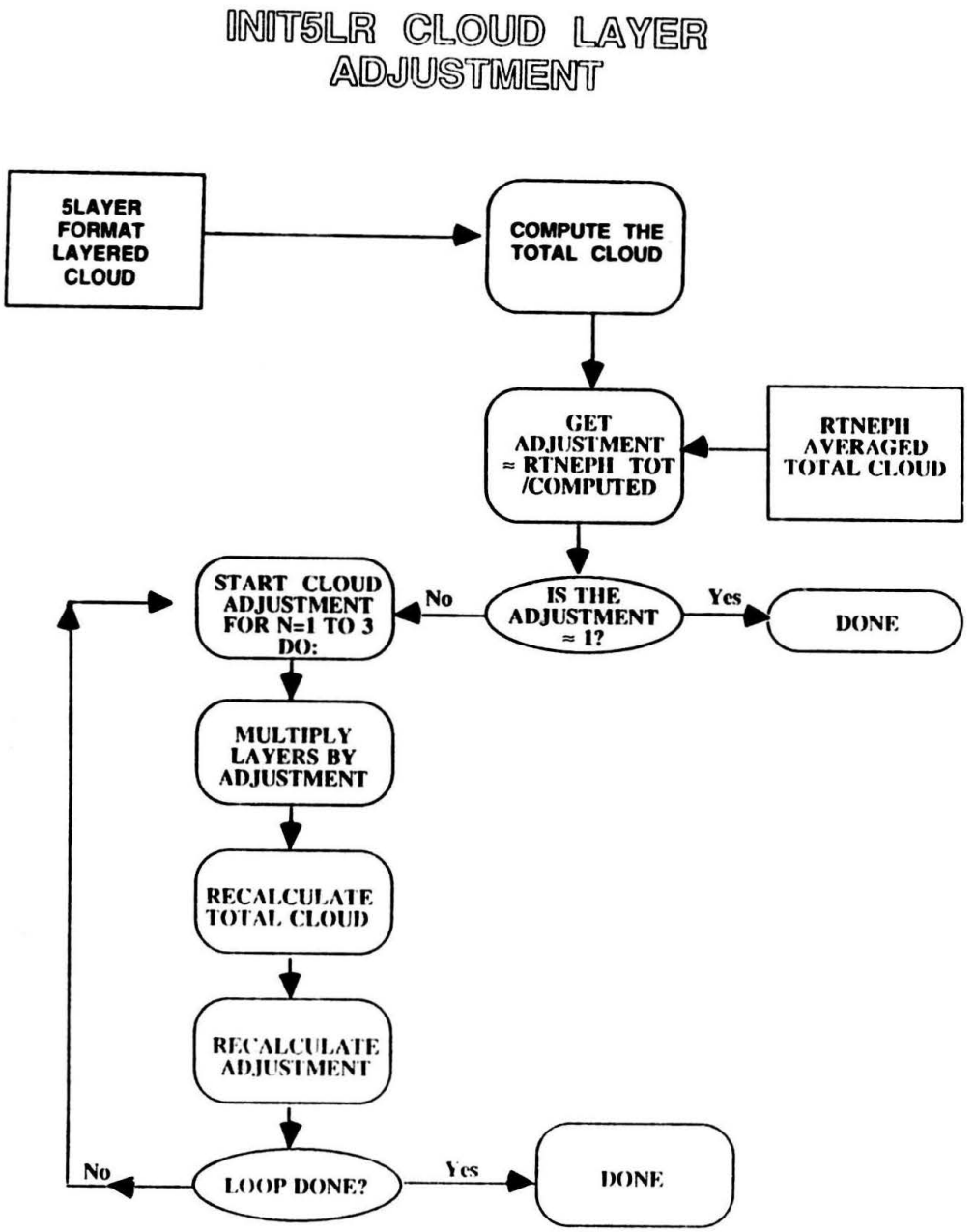

Fig. 6. Logic flow for adjusting the layer cloud amount spread to the five layers in 5LAYER to make the computed total cloud amount near the observed total cloud amount.

$$CPS = [\ B_0(P) + B_1(P) * DPD\ ] * DPD \qquad (4)$$

where

$$B_0(P) = B_{00} + B_{01} * P$$
$$B_1(P) = B_{10} + B_{11} * P$$

and

$$B_{00} = 1.41985$$
$$B_{01} = 1.34466E\text{-}2$$

$$B_{10} = -1.39131E\text{-}2$$
$$B_{11} = -6.69419E\text{-}5$$

The resulting error is less than 4%, when compared with an exact conversion.

Now that the relationship between CPS and dew-point depression has been established, it remains to relate CPS to cloud amount. Intuitively, small values of CPS (small dew-point depressions) correspond to large values of cloud amount, and, conversely, large CPS values (large dew-point depressions) correspond to small cloud amounts. Edson (1965) presented empirical curves relating these two variables. These empirical curves are shown in Figure 7 and tabulated in Appendix B.

There are several advantages to using CPS as the moisture parameter. First, as previously discussed, CPS provides the link between dew-point depressions and cloud amounts required for initialization in cloud and cloud-free areas. Second, CPS also links changes in cloud amount to changes in vertical motion. For example, should an unsaturated parcel of air be lifted, adiabatic cooling takes place. Simultaneously, the dew-point depression narrows, and additional clouds form. For descending motion, the air becomes drier, and clouds dissipate. Therefore, cloud amounts in terms of CPS (units of pressure) can be modified directly by the net vertical displacement (units of pressure) of a parcel of air.

2.2.3.2 Moisture in clear areas.

Initialization schemes up to this point have determined CPS in areas where clouds exist. However, CPS values have not been adequately described in cloud-free regions. For example, a volume of air with no cloud may be very dry or it may be so moist as to require only minimum adiabatic cooling to begin cloud formation. The RTNEPH cloud information cannot define moisture in cloud free regions. Consequently, for these regions we turn to an alternate data source.

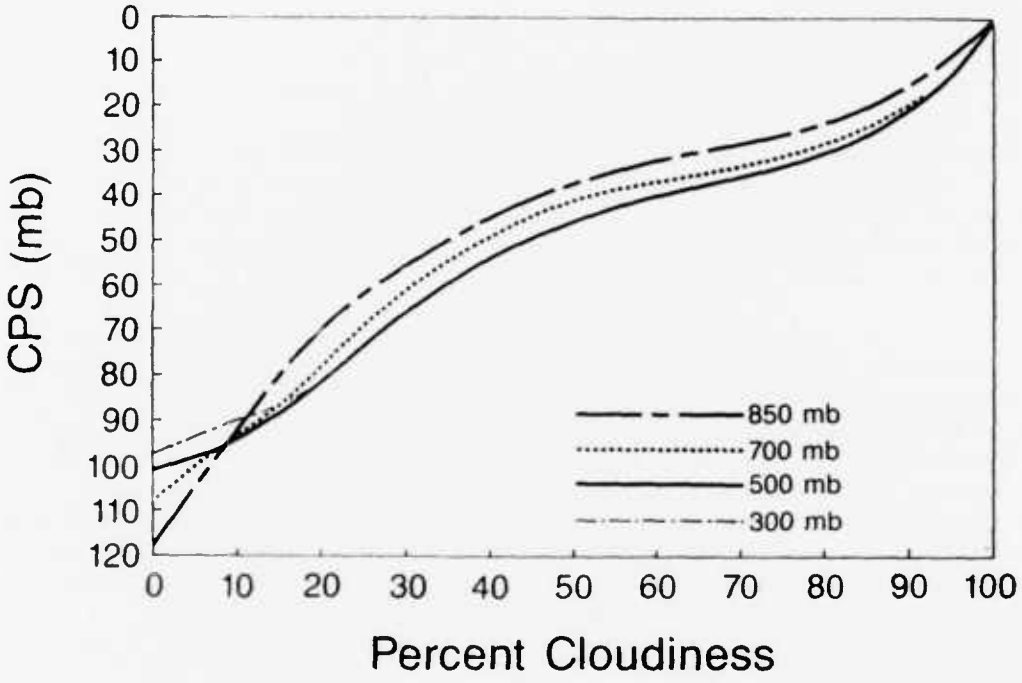

Fig. 7. Empirical relation between condensation pressure spread (CPS) and percent cloud amount at four pressure levels. After Edson (1965).

To provide this information, a dew-point depression analysis from the AFGWC Multi-level Analysis Model (Tarbell and Hoke, 1979) is used. The initialization scheme creates the half-mesh (100 nm) field by interpolation from whole-mesh values as described in Appendix C.

This three-step initialization process is summarized by the flow diagram in Figure 3. First, the half mesh analysis is constructed using RTNEPH values in cloudy areas. Secondly, the dew-point analysis in cloud-free regions is determined from the conventionally analyzed dew-point depression values. Then a check is made to ensure that the drier of the analyzed dew-point depressions or cloud-to-CPS conversion is used.

However, a problem has been created in that the moisture field in the initialization scheme consists of both cloud information (in percent cloud average) and dew-point depressions (in degrees). A common moisture parameter needs to be specified. This parameter, condensation pressure spread (CPS), links cloud amount and dew-point depression.

2.3 Temperature Initialization

If temperature, or any parameter requiring it, is forecast, an initial temperature field is required. At AFGWC this field is created by the High Resolution Analysis System (HIRAS). The HIRAS derives temperatures from the geopotential thickness between two pressure levels at six levels (1000 mb, 850 mb, 700 mb, 500 mb, 400 mb, 300 mb). These temperatures are converted to a whole-mesh (200 nm) grid spacing.

Some modification of this information is required to format it in the five level, half-mesh (100 nm) grid system of 5LAYER. Whole-mesh temperatures are horizontally interpolated to half-mesh in the same manner as dew-point depressions (recall section 2.2.3.2.) The four required pressure levels correspond to pressure level information from the analysis model directly. However, initialization of temperature on the terrain-following (gradient) level requires additional information extraction techniques. No attempt is made to use surface temperature values. Rather, gradient level temperatures are assigned based on standard pressure level information.

The gradient level is initialized by height interpolation between fixed pressure levels. This technique ensures a representative value of temperature is assigned. Gradient temperatures are thus relatively free from local, small-scale temperature effects.

3. TRAJECTORY COMPUTATION

3.1 General Motivation

Cloud and temperature forecast models at AFGWC are for the most part diagnostic in nature. However, dynamic properties that do exist are found implicitly in the trajectory computation. Wind forecasts from the GSM are used to construct three-dimensional trajectories to determine the path of an air parcel. The input data for trajectory computation consists of GSM-derived whole-mesh wind forecasts at three-hour intervals for the 1000 mb, 850 mb, 700 mb, 500 mb, and 300 mb pressure levels.

By averaging the wind forecasts in time, the trajectories are computed backward from selected terminal points (grid points) to origin points. Since these trajectories determine the origin of an air parcel, they are computed by starting at the final forecast point. The model calculates an "upstream" trajectory in three-hour intervals until the parcel's origin is determined. From these points, analyzed atmospheric elements such as clouds and temperatures can be displaced and modified as each parcel traverses its trajectory path. Figure 8 shows a conceptual flow chart of the trajectory computation process.

Very critical to the accuracy of these origin points is the choice of approximations to the wind field. Using different geostrophic or stream-function approximations, Djuric (1961) showed that in only 12 hours the average displacement error of the origin point ranges up to 20% of the trajectory length. Therefore, the forecast accuracy of any meteorological element (clouds and temperatures) is extremely dependent upon the accuracy of the wind model. In an extreme case, it is conceivable that the movement of a trough or ridge pattern could be so fast or so slow as to cause the forecast elements to be 180° out of phase.

Experiments were conducted in 1974 at AFGWC to quantify the effect of wind model errors on forecast accuracy. Because trajectory origin points are difficult to verify, the experiments were designed to verify the accuracy of a forecast element such as clouds. One particular experiment compared cloud forecasts which were produced from three wind models. One was a baroclinic, quasi-geostrophic model, another was a primitive equation (PE) model and the third was a "perfect prog" model that uses successive wind analyses. Overall, the cloud verification showed that the wind model accounts for 25% of the standard deviation of error (STDE). The other 75% was attributable to grid-associated shortcomings, variance attributable to wind and cloud analyses, and cloud forecasting algorithms. Of particular note was the superior performance of the PE model over the quasi-geostrophic model. The STDE's for the PE driven cloud forecasts showed a 25% improvement. Therefore, it was desirable to link the trajectory computations to the AWSPE model which provided the best operational wind forecasts at AFGWC. The GSM succeeded the AWSPE in October 1985. With the advent of larger computers and more sophisticated wind models, the future offers great potential to increase not only trajectory accuracy but also forecast element accuracy.

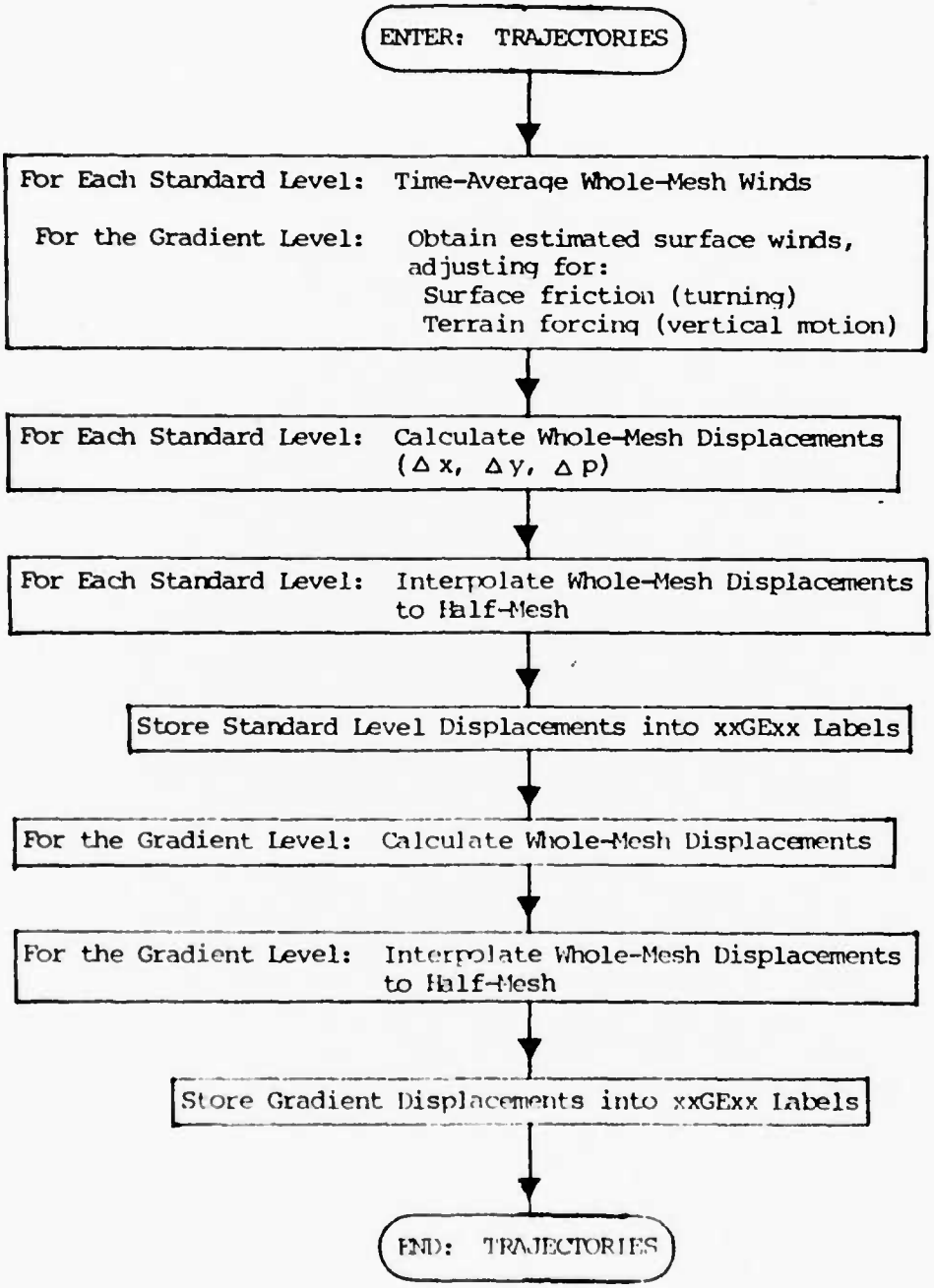

Fig. 8. Flow of steps taken to compute 5LAYER trajectories from forecasts of GSM wind components.

3.2 Pressure-following Levels

To compute trajectories, the model uses an unpublished technique developed by Mr Ralph Jones (currently at the National Meteorological Center). The method involves using a Taylor series expansion about a grid point to compute representative wind components u, v, and ω. For the u component, the equation takes the form

$$u_s = u_e + \frac{\partial u_e}{\partial x} dx + \frac{\partial u_e}{\partial y} dy + \frac{\partial u_e}{\partial P} dP \tag{5}$$

where u_e and u_s refer to the u-components at the grid point and trajectory origin, respectively. Derivatives on the right-hand side are approximately three-hour average changes. By assuming

$$\bar{u} = (u_e + u_s)/2 \tag{6}$$

and substituting (5) into (6) for u_s, one obtains

$$\bar{u} = u_e + \frac{1}{2} \left[\frac{\partial u_e}{\partial x} dx + \frac{\partial u_e}{\partial y} dy + \frac{\partial u_e}{\partial P} dP\right] \tag{7}$$

Trajectory displacement components are then computed from

$$\Delta x = -\bar{u}\Delta t \tag{8}$$

The advantage of using the partial Taylor series method is that trajectory displacements represent curvature in the flow more adequately than iteration techniques. Appendix D gives a detailed, explicit solution to (7), as well as comparable derivations for the v and ω wind components.

3.3 Gradient Level

Trajectory displacements are also computed in the terrain-following gradient level. Computations here are basically the same as those that are described in section 3.2. However, the evaluation of the derivatives in (7) at this level needs further explanation. Also, because the gradient level is a terrain-following level, special terrain adjustment features are inherent to the trajectory calculations and need to be explained.

In order to evaluate the horizontal and vertical derivatives in (7) with respect to the gradient level, a wind field at this level is required. Since such a field does not normally exist, it is created by linear vertical interpolation between known wind components above, and terrain-level (surface) components below the gradient level. The components above the gradient level come directly from the next pressure level. However, the surface-level winds may or may not be used in a direct manner. This decision is based on whether the terrain pressure height is above or below 1000 mb. If the pressure height is equal to or greater than 1000 mb, the 1000 mb wind components from the GSM are used directly. However, if it is less than 1000 mb, then the two closest pressure levels are vertically interpolated to calculate u_t and v_t. In either case, these two components are modified to account for surface friction. The velocities are modified by a roughness turning angle ranging from eight degrees over water to 20 degrees over rough terrain.

The vertical, terrain-level, wind component, w_t, is needed for vertical interpolation to the gradient level. This terrain induced motion is approximated by:

$$w_t = -100\left(u_t \frac{\partial h}{\partial x} + v_t \frac{\partial h}{\partial y}\right) \tag{9}$$

where h is the terrain height in meters. The -100 term in (9) is an approximation to convert the vertical velocity from 10^{*}m/s to 10^{4*}mb/s. This scaling preserves consistency with vertical wind components at the pressure levels. Now that all wind components above and below the gradient level are known, u_g, v_g, and w_g are determined by vertical interpolation. Equation (14) uses these newly derived components to produce terrain-following trajectories.

3.4 Boundary Characteristics

3.4.1 Terrain Effects

Because of its proximity to the surface, gradient-level wind components may be modified to account for steep terrain conditions. This terrain field is extracted from the RTNEPH, but it is modified to a half-mesh (100 nm) format by using a 25-point unweighted average.

Modification of the gradient-level trajectories for terrain effects is done for two practical reasons. The first is to prevent an upstream trajectory from backing into the terrain. This limitation avoids calculation of trajectories that have origins which are below the terrain surface. At the conclusion of each time step, the pressure of the trajectory origin is compared to the interpolated terrain pressure. If the origin intersects or is below the terrain level, the vertical component of the trajectory is adjusted so that it is exactly 20 mb above the terrain pressure height.

A second limitation to these wind components is the restriction of extremely large values of dP/dt that are terrain induced. After repeated experiments it was determined that vertical displacements of 50 mb/3 hr or larger produce undesirable effects. These large vertical displacements lead to copious amounts of precipitation in areas of steep ascent, with compensating areas of extreme dryness on the descent side. Additionally, large values of upward motion aggravate an inherent tendency toward dryness in the cloud model. This aridity is caused primarily by the lack of low-level moisture sources, such as the Gulf of Mexico, being included in the model.

To correct these deficiencies, the vertical displacement at each grid point is checked for values greater than 50 mb/3 hr. When this criteria is exceeded, each of the horizontal trajectory components is halved. A new vertical displacement is computed from these shortened trajectories, and this process is continued until the extreme values of DP/dt are reduced below the 50 mb/3 hr criteria.

3.4.2 Lateral Effects

The horizontal grid on which these calculations are made is superimposed on a Northern and Southern Hemispheric polar-stereographic map projection. The orientation of the grid system on the map projection is such that 10°E and 170°W longitudes are parallel to the x-axis. Figures 1 and 2 show the two hemispheric projections and the lateral boundary of the grid system. Generally, the area that is inscribed by this octagon-shaped lateral boundary is poleward of 10° latitude excluding most of the Tropics. The model computes trajectories for all grid points that are internal to this boundary.

The prime lateral constraint on the trajectory computations is to prevent origins from being outside the octagon (lateral boundary). Generally, all trajectories within two whole-mesh (200 nm between grid points) grid points are checked to insure that this condition is preserved. Specifically, the actual constraint depends upon the trajectory's proximity to a particular boundary. For the grid rows and columns that are adjacent to the boundaries that are parallel to the x- and y-axes, the model does not permit x's and y's that are outside the boundary. Those parcels originating outside the lateral boundaries are truncated to the lateral boundary.

Implementation of this truncation concept near diagonal boundaries is more complicated. The following mathematical section formally describes the system used. Conceptually, the diagonal is rotated 45°, the truncation concept is applied and then the diagonal is rotated back to the initial orientation. While the math appears difficult, the results are straightforward.

In order to restrict the trajectory origins that are computed in the vicinity of the diagonal boundaries, a modified x,y-coordinate system needs to be established. First, a unit vector perpendicular to each of the diagonal boundaries is defined. Using Figure 9 and geometric considerations the unit vector $\vec{u}$ can be specified in terms of $\vec{i}$ and $\vec{j}$ as:

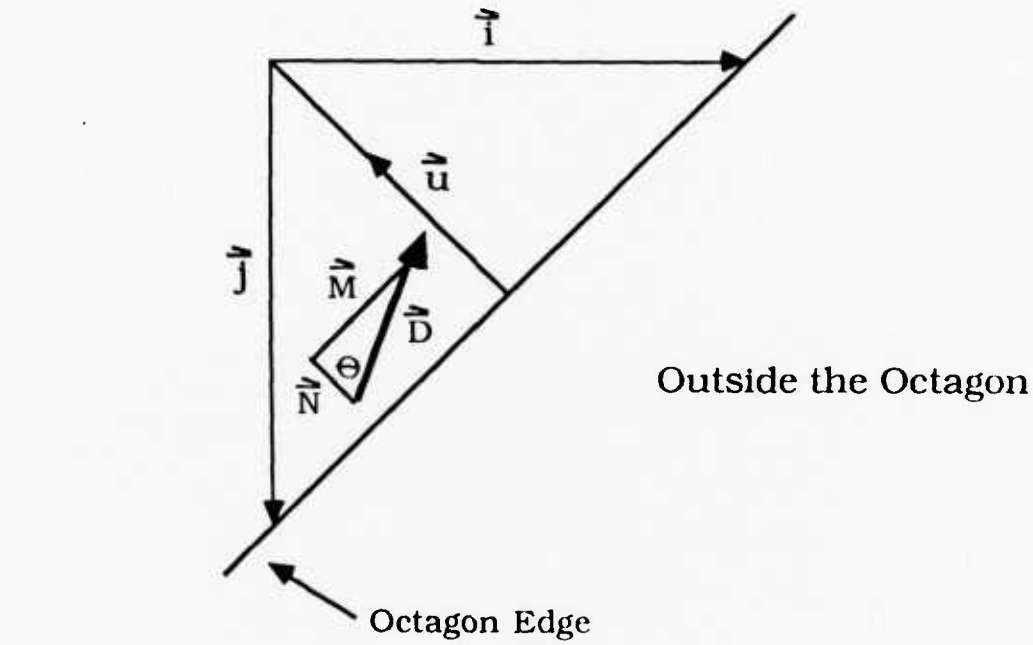

Fig. 9. Geometric considerations near the diagonal lateral boundaries.

$$\vec{u} = \pm 0.7071\ \vec{i} \pm 0.7071\ \vec{j} \tag{10}$$

where $\vec{i}$ and $\vec{j}$ are unit vectors parallel to the x- and y-axes respectively and the +/- signs determine which of the four diagonal boundaries is being considered. To determine if the horizontal vector $\vec{D}$ has a component that is along $\vec{u}$ and directed inward, the angle between $\vec{u}$ and $\vec{D}$ is calculated. Since, by definition

$$\vec{u} \cdot \vec{D} = |\vec{u}|\ |\vec{D}|\ \cos\theta \tag{11}$$

and

$$\vec{D} = \Delta x\vec{i} + \Delta y\vec{j} \tag{12}$$

then, substituting for $\vec{u}$ and $\vec{D}$, the formula for cos θ is:

$$\cos\theta = \frac{0.70711(\pm x \pm y)}{(x^2 + y^2)^{1/2}} \tag{13}$$

Therefore, if $\vec{u}\cdot\vec{D}$ is greater than zero, then cos θ is greater than zero and $\vec{D}$ has a component along $\vec{u}$ and directed inward. If this criteria is not met, then $\vec{D}$ is modified by subtracting the value of the normal to the edge of the octagon component that is parallel to $\vec{N}$. This component, $\vec{N}$, is defined as:

$$|N| = |D|\ \cos\theta \tag{14}$$

substituting for cos θ from (11), $\vec{N}$ is:

$$\vec{N} = \left[\frac{\vec{u} \cdot \vec{D}}{\vec{u} \cdot \vec{u}}\right] \vec{u} \tag{15}$$

Using (12) for $\vec{D}$ and (15) for $\vec{N}$, the component of $\vec{D}$ parallel to the diagonal boundary $\vec{M}$ is calculated from the vector subtraction

$$\vec{M} = \vec{D} - \vec{N} \tag{16}$$

The horizontal components of the three-dimentional trajectory are set equal to the value of $\vec{M}$. The effect of these lateral constraints is to permit flow parallel to the boundary and parcel origins that are internal to the grid system, while eliminating flow from outside the boundary. Classically this situation has been described as a free-slip, non-permeable boundary condition.

4. FORECASTING

The forecasting of temperature and moisture is accomplished after the initial fields of these parameters and the forecast trajectories are determined. Despite the detail in the following subsections, the general methodology of a Lagrangian advection scheme is simple. This scheme uses trajectories obtained from wind forecasts to determine the origin of an air parcel. The initial value of some weather element associated with this air parcel is determined. Then, the initial value is modified as the parcel traverses the path of the trajectory. The following subsections discuss certain atmospheric processes which influence the temperature and moisture content of an air parcel during its journey.

4.1 Moisture

The forecasting techniques applied to CPS consider those atmospheric processes which greatly affect cloud formation and dissipation. Condensation pressure spread can be modified by horizontal advection as well as vertical advection. In addition, entrainment is especially important near the boundaries of air masses. Formulations have been developed at AFGWC to diagnose favorable entrainment situations and then to parameterize this effect. Another cloud producing mechanism which must be considered is solar heating of the Earth's surface.

One of the observable effects of the heating cycle is the diurnal increase in cloudiness over land by day and subsequent decrease at night. Details of this process and its simulation will be discussed later. Finally, clouds are influenced by moisture source regions as they traverse open water. The effects of precipitation and evaporation on cloud formation will be discussed in a later subsection.

4.1.1 Horizontal Displacement

The numerical characteristics of the forecasting routines can have a large effect on the cloud forecasts. Trajectory origins are computed for each grid point at every time step. The interpolation scheme used to define the value of the weather elements to be forecast at these origins is very important because it is applied each time step. Any inherent error in the scheme contributes additively to forecast inaccuracy.

Selecting the interpolation scheme that introduces the least error is not a simple task. Most schemes assume that a parameter varies continuously between known values. Linear interpolators assume linear variation. Bessel interpolators compute the gradient (first derivative) and the rate of gradient change (second derivative) to determine the unknown value. The discontinuous distribution of clouds in the atmosphere makes the application of interpolators to cloud fields very difficult.

Despite this difficulty, a two-point and an eight-point linear interpolator are used in 5LAYER. Each of these interpolators are shown in Figure 10. The two-point interpolator rounds the origin location to the nearest grid point. Linear interpolation is done between the closest pressure-following levels as shown in Figure 10A. The two-point interpolator can be rapidly computed; however, its accuracy is reduced because of rounding the trajectory length. The eight-point interpolator reduces this inaccuracy by maintaining the proper trajectory length (see Figure 10B). However, it is a costly computer routine because interpolation is applied at each grid point (9393 grid points per level), at each level, and at every time step.

The 5LAYER model combines these two interpolators in order to derive benefits from each. The two-point interpolator is used at a point when the cloud analysis has 50 percent or less cloud coverage. The eight-point scheme is used if the analysis has greater than 50 percent coverage. The benefits are a precise description of large cloud coverage (greater than 50 percent) and reduce computational time. Combining these two interpolators causes different cloud advection rates. Scattered cloud coverage (50 percent or less) will not be advected at the same rate as broken or overcast coverage (greater than 50 percent). This effect is not considered a serious problem. Rounding trajectory lengths over many time steps reduces this error source since some trajectories will be lengthened and others shortened.

4.1.2 Vertical Displacement.

The effect of vertical motion on cloud formation is not thoroughly understood. Unsaturated rising air cools due to adiabatic expansion until water vapor condenses to form clouds. Conversely, adiabatic compression dries air parcels until droplets disappear. To simulate this process, the vertical trajectory component, Δp, is applied directly to the CPS value. This is described by

$$C_F = C_I + \Delta p \tag{17}$$

where C_F is the forecast CPS value and C_I is the initial CPS value. The value of C_I is determined at the trajectory origin by three-dimensional interpolation of the initial CPS field. In (17) rising motion (negative p) when applied to the CPS analysis, produces larger cloud amounts and smaller CPS values. The convenience of representing clouds in terms of units of pressure is again obvious.

There are some limitations in the application of (17). After advection along the trajectory, C_F is limited to be greater than or equal to zero. Negative values would indicate supersaturation, in such cases the excess moisture is condensed and added to the quantitative precipitation.

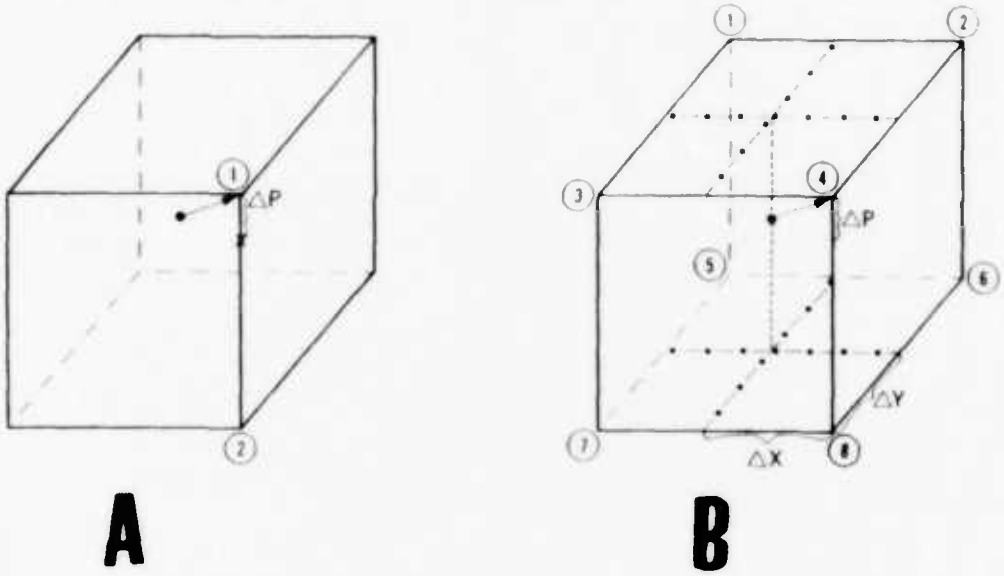

Fig. 10. Two-point interpolation (A) and an eight-point interpolation (B).

4.1.3 Entrainment

One problem of true Lagrangian advection is that there can be no interaction between parcels. In an attempt to parameterize this interaction, a scheme was developed to mix environmental air with the cloud mass. Entrainment is especially needed near the edges of clouds and cloud-free regions where modification due to mixing is strong.

The model simulates two types of mixing. The first is general entrainment applied to all grid points while the second is a more specific formulation that is applied primarily at cloud edges. The general entrainment provides for large-scale mixing of moving cloud systems. This simulation modifies the CPS value that arrives at the terminal point of the trajectory by applying the CPS that existed at the grid point in the previous time step. The general entrainment is given by

$$C_m = (3C_F + C_p)/4 \qquad (18)$$

where C_p is the CPS at the grid point from the previous time step, C_F is the forecast CPS, and C_m is the final, mixed CPS. This technique typically works well for the advection of large-scale cloud systems into arid, desert regions such as the Sahara Desert where, without this technique, clouds are forecast more frequently than observed.

A disadvantage of this technique is that, in time, the cloud boundaries tend to lose their distinct edges. To counteract this effect, a more specific entrainment method was developed to preserve well-defined cloud boundaries. The intent of this procedure is to emphasize the importance of vertical motion to cloud formation or dissipation; the method has been researched and emphasized by Edson (1965). This technique is more limited because it is applied only when descending parcels cause cloud-free grid points to become cloudy or when ascending parcels cause cloudy points to become clear. This situation is represented in Figure 11. The methodology of this procedure is to first diagnose whether the specific conditions are occurring and second to apply an appropriate "wet" or "dry" weighting factor. If a cloud-free grid point becomes cloudy while undergoing descending motion, then an area-weighted state of dryness is calculated. Based on the actual number of horizontally adjacent cloud-free grid points and the strength of the descent, the drying of the cloud parcel is forced to accelerate. In a similar manner, should a cloudy grid point become clear while undergoing rising motion, the surrounding moisture and the upward motion are used to accelerate cloud formation. As intended, this procedure emphasizes the effect of vertical motion on cloud formation.

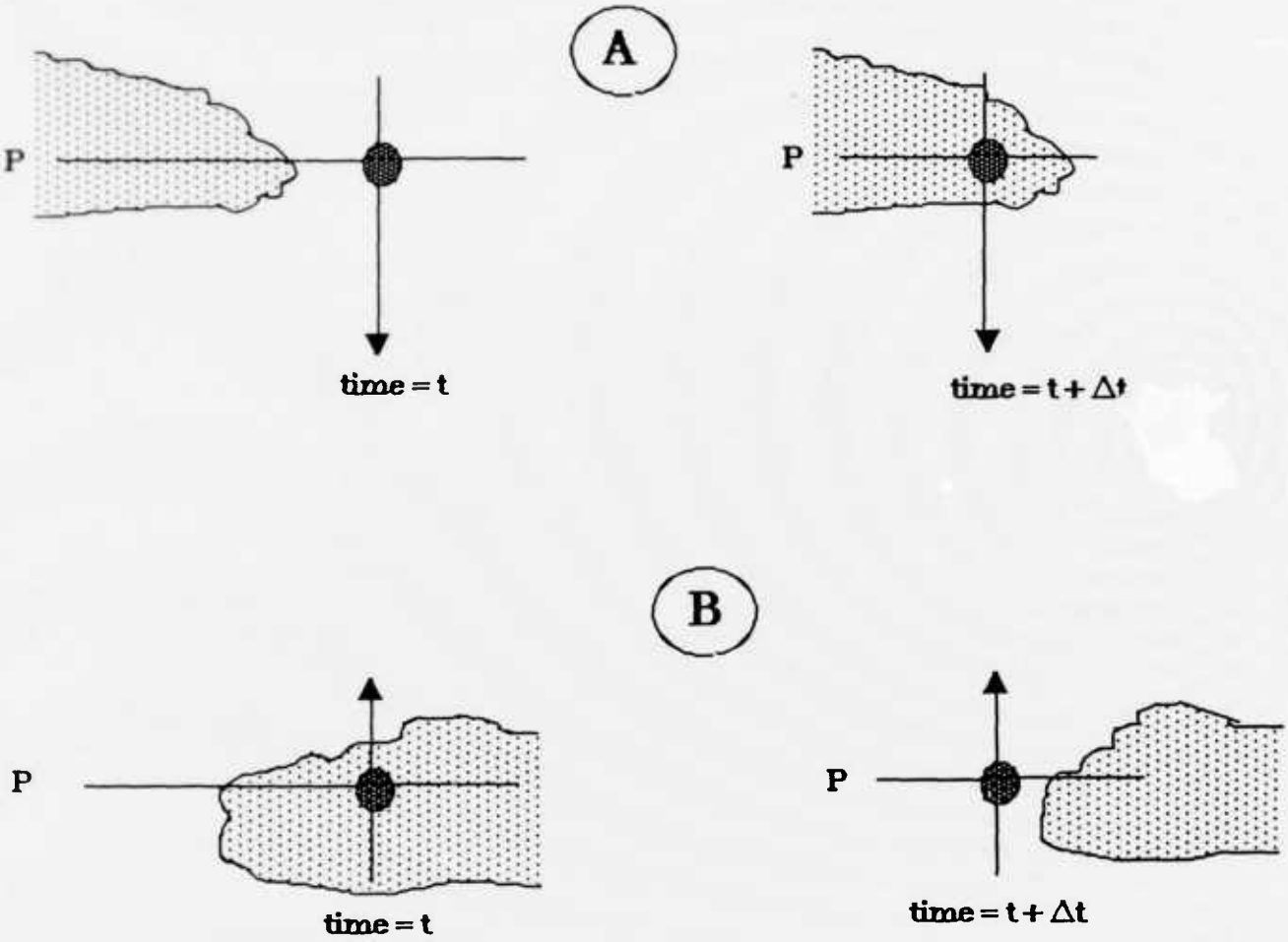

Fig. 11. Situations for entrainment near cloud boundaries. In A, the grid point becomes cloudy at the time t + Δ t under descending motion. In B, clearing is associated with rising motion.

4.1.4 Diurnal Effects.

Another important cloud producing mechanism is the diurnal solar heating cycle. With the correct proportions of moisture and solar heating, air parcels rise from the surface, cool adiabatically, and, if the lifting condensation level is reached, form clouds. This mechanism is especially important during the summer months when heating is strong and horizontal advection is weak. Because of the parameterization procedure described in the following paragraphs, not only is the solar heating mechanism incorporated, but also any persistant localized effects such as those caused by steep terrain features.

The diurnal cloud-forecasting technique involves maintaining a two-day average value of CPS at each base time (0000 GMT plus every three hours) and for every grid point. Therefore, the difference between two of these fields at a grid point represents a diurnal change of CPS. Since each mean field has a specific base time, then the diurnal change is valid over that period. For example, if the 0000 GMT field is subtracted from the 0300 GMT field, then the difference represents the diurnal fluctuation of clouds over that time period. Since these fluctuations are calculated for each grid point, local effects are also incorporated.

However, the strength of the diurnal effect may be weak compared to other meteorological effects. For example, advection of clouds may be the major factor that determines a cloud forecast, with diurnal effects having a minor role. In order to diagnose the relative strength of the diurnal effect, each point of the current analysis is compared with the equivalent points of the corresponding mean field. Based upon the amount of disagreement between the current analysis and the associated running mean field, a weighting factor ranging from one to zero is assigned. If the analysis and the mean field are very similar at a point, a weighting factor of 1.0 is assigned and the total diurnal effect is incorporated. Smaller and smaller weight factors are assigned to each point as differences between the current analysis and the mean field increase. A zero weighting factor is assigned if the difference between the analysis and the mean field exceeds a previously established upper limit. For CPS, the value of this criteria varies due to the non-linear relationship between cloud and CPS, as shown in Figure 7. For example, changes in percent cloudiness in the middle ranges of cloudiness represent smaller changes in CPS than cloudiness changes at either end of its spectrum. In general, the diurnal parameterization is not applied if the difference between the mean and analyzed fields is greater than 30 percent change in cloudiness.

4.1.5 Evaporation of Precipitation

Lastly, CPS can be modified by simulating low-level evaporation of liquid water that falls from upper layers. Liquid water amounts are in the form of a quantitative precipitation forecast (QPF). A discussion of this QPF calculation is in section 4.3.4.

The simulation of low-level evaporation of falling precipitation is based on two observed conditions that affect evaporation rates. First, very dry air produces an evaporation rate greater than moist air. Second, relatively large amounts of liquid water available for evaporation cause high evaporation rates. These conditions can be quantified so as to produce new values of cloudiness. If Q_1 represents the amount of QPF falling into a layer (inches per 3 hours) and C_1 is the initial CPS, then the new CPS, C_2 is calculated using

$$C_2 = C_1 - (C_1 Q_1) \tag{19}$$

The subtraction of the product in (19) is necessary since low values of CPS represent high values of cloudiness. In addition, should Q_1 equal one inch per three hours, then C_2 becomes equal to zero; this represents total overcast conditions. Therefore, Q_1 is limited to values no greater than one. Should this condition occur, the value of cloudiness at the grid point is set to be overcast, and the remainder of the QPF is allowed to "fall out." this remaining QPF, Q_2, is determined by

$$Q_2 = Q_1 - (Q_1 (C_1 - C_2)/C_1) \tag{20}$$

Comparing (19) to the two observable conditions stated above shows that these conditions are now specified. Equation (19) allows large changes in CPS (greater evaporation) when either large values of C_1 (dry air) or large values of Q_1 (large amounts of liquid water) are observed. Equation (20) shows that the amount of QPF falling through the layer is proportional to the percentage change in the CPS at the point. This equation is necessary in order to determine the amount of liquid water available for evaporation in lower levels and to determine the actual precipitation amount reaching the ground. Both of these equations are applied to the two lowest grid levels, 850 mb and gradient.

4.2 Temperature

A Lagrangian method for advection is used to forecast temperature, as well as to forecast CPS values. To produce a forecast, the temperature at the initial point of a trajectory is determined by three-dimensional interpolation in the initial temperature field. As the trajectory displaces the parcel, several atmospheric processes are simulated to modify this initial temperature value. The dry adiabatic process is the most important, at least over periods of two days or less. Other important effects on temperature forecasts, but

secondary, are the effects of latent heat release, diurnal heating, and turbulent mixing. Finally, in order to maintain vertical consistency, the temperature lapse rate at each point is checked to insure that superadiabatic lapse rates have not been created. Section 4.2.5 describes how superadiabatic conditions are handled.

4.2.1 Dry-Adiabatic Process

The first law of thermodynamics for adiabatic processes indicates that no heat is added to or taken away from an air parcel during ascent or desent (a reversible process). This formulation, known as Poisson's equation, is written as

$$T_F = T_I \quad (P_F/P_I)^{0.286} \tag{21}$$

where T_F is the temperature at the termination of the displacement, T_I is the temperature at the origin of the displacement, and P_F and P_I are pressure values at the termination and origin of the displacement. The value of P_F is always the pressure level for which a forecast is being made, for example, 300 mb. The exponent, 0.286, is the ratio R/C_p where R is the specific gas constant for dry air, and C_p is the specific heat capacity at constant pressure.

4.2.2 Pseudo-Adiabatic Process

Whenever an air parcel changes phase (melts, freezes, evaporates, condenses, or sublimes), a quantity of heat must be supplied to or taken away from the parcel. This heat warms or cools environmental air at a rate that differs from the dry adiabatic (reversible) process. To simulate this pseudo adiabatic effect on the temperature of saturated parcels, a technique using an approximate solution has been developed. The ultimate goal of this technique is to find the temperature of a parcel that terminates at the final forecast level, P_F, after it has gone through a moist expansion process.

The approximate solution assumes linear rates of change of wet bulb potential temperature with pressure. This eliminates the need for exponentiation (an expensive computer operation) and produces accurate results for the relatively small vertical displacements typical of three-hour time steps.

4.2.3 Entrainment.

As stated in Section 4.1.3, there needs to be some mechanism to allow parcels of air to interact. For temperature, this is especially critical for two situations where thermal mixing is a significant effect. One involves mixing over water, and the other low level, turbulent mixing.

The importance of temperature modification of air masses as they move over large water sources has been well established. A study by Reap (1971) reports the importance of this modification and describes an empirical expression that forecasts air temperatures over water regions. To produce an air temperature forecast, this expression combines three-fourths of the final sea-surface temperature plus one-fourth of the initial air temperature. After experimenting with several proportions at AFGWC, the following parameterization for air-sea temperature interaction was selected

$$T_M = (3T_F + T_P)/4 \qquad (22)$$

where T_P is the temperature at the grid point from the previous time step, T_F is the forecast temperature, and T_M is the final, mixed temperature. This expression is applied at all levels for all grid points over water.

Another temperature modification simulates the effects of low-level, turbulent mixing. The intent of this procedure is to diagnose conditions favorable to this mixing and then apply the mixed condition. One such condition that is favorable for this mixing is parcels descending to the gradient level. Instead of computing an adiabatic change to this level, the standard atmospheric lapse rate for the troposphere is used (5.9 K/100 mb). This lapse rate is less than the adiabatic one. Therefore, parcels descending to the gradient level are cooler than if they descend at the adiabatic rate. The selection of the standard atmospheric lapse rate is solely based on its ability to produce gradient-level temperatures that are cooler than those produced by an adiabatic lapse rate.

4.2.4 Diurnal.

Temperature forecasts are also modified by local diurnal effects. The method to produce these effects is essentially the same method as that used to diurnally modify CPS values (recall Section 4.1.4). Two minor variations of this method need to be noted. First, the mean temperature field is maintained for eight days instead of two. Second, the upper limit that determines whether any diurnal effects are to be applied is set to 283 K. These two values have been established after an extensive statistical evaluation of temperature forecasts.

4.2.5 Superadiabatic Lapse Rate Modification.

Forecast temperatures are altered when the advection process creates superadiabatic lapse rates. These lapse rates are eliminated by adjusting the forecast lapse of temperature. Kliminating superadiabatic lapse rates is justified since they rarely would be observed and only for short durations. The general procedure to remove a superadiabatic layer is to determine the lapse rate between two pressure levels. If this rate is superadiabatic, then the upper level is warmed and the lower level is cooled. This warming and cooling is done in small increments, and the sounding is continuously checked to ensure that no superadiabatic lapse rates are created at other levels by this adjustment procedure.

4.3 Derived Quantities

Temperature and CPS are the only meteorological elements that are advected by this forecasting scheme. However, additional elements may be derived from forecasts of them. These non-advected, secondary forecast fields include layered and total cloud cover, dew-point depression, stability, quantitative precipitation forecasts, cloud type, and icing. The following sections describe the methodology that is used to obtain these derived fields.

4.3.1 Layered and Total Cloud Cover

Layered cloud forecasts are derived from forecast CPS fields using tables (Appendix B) that convert CPS to cloud amounts. From these layered cloud forecasts, a total cloud field is created by the technique discussed in Section 2.2.2.

The choice of CPS as the advection element for cloud forecasting is not a simple one. For example, primitive equation forecast models that incorporate moisture can initialize and forecast a moisture related element such as specific humidity or dew-point depression ($T-T_d$). Areas of clouds are then inferred from these moisture fields. In fact, early cloud forecasting models at AFGWC used dew-point depression to infer cloud amounts. To determine which meteorological element produces the most realistic cloud forecast, an experiment was conducted at AFGWC during the summer of 1974 contrasting CPS and dew-point depression.

The experiment consisted of independently initializing, forecasting, and verifying dew-point depressions and CPS. An automated verification program compared the following criteria: forecasts and observations of dew-point depressions, forecasts of CPS (converted to dew-point depression) to observations of $T-T_d$, forecasts of CPS to observed clouds, and forecasts of dew point depression to observed clouds. While the statistical results of

this experiment are not available, the qualitative results were summarized as follows: In verifying dew-point depression forecasts against station observations of dew-point depressions, advected MULTAN dew-point depressions (a scheme that initializes and forecasts dew-point depressions) shows more skill almost everywhere than CPS (a scheme that initializes and forecasts CPS). However, advected MULTAN dew-point depression forecasts are poorly correlated with cloudiness. Because of these results and the operational requirement for a cloud forecasting model, CPS was chosen to be the advectable moisture element in this forecasting scheme. Since CPS is the only advectable quantity, the verification statistics should correlate well with cloud observations but not with dew-point depressions. Even though forecasts of dew-point depression are produced, they are, in fact, derived from forecasts of CPS using the method described in the following section. Users of AFGWC dew-point depression forecasts should be aware of the procedures that derive these forecasts.

4.3.2 Dew-Point Depression

Forecasts of dew-point depression (DPD), $T-T_d$, are produced directly from the forecast CPS values. The equation for the conversion from CPS to DPD is:

$$DPD = CPS \; / \; [A_0(P) + A_1(P) * CPS \,] \qquad (23)$$

$$A_0(P) = A_{00} + A_{01} * P$$
$$A_1(P) = A_{10} + A_{11} * P$$

where

$$A_{00} = 1.46917$$
$$A_{01} = 1.36305E\text{-}2$$

and

$$A_{10} = -9.01177E\text{-}3$$
$$A_{11} = 1.7772\ E\text{-}6$$

The resulting error is less than 5%, when compared with an exact conversion.

4.3.3 Stability

Using temperature and moisture forecasts, a measure of the atmosphere's static stability can be determined. For those grid points that have a terrain height below the 850 mb level, a standard Showalter Stability Index (Huscke, 1959) is computed. Using the 850 mb temperature and dew point, the parcel's pressure and temperature at its lifted condensation level (LCL) is determined. The parcel at the LCL is lifted moist adiabatically to 500 mb where the parcel's temperature is compared to the 500 mb environmental temperature. The difference between these two temperatures is the Showalter Stability Index. The moist adiabatic computation is the one mentioned in Section 4.2.2.

When the terrain is above 850 mb, a different, more empirical approach is taken. Based upon observational evidence, a technique that produces a continuous field of stability indexes in a steep terrain region is used. It was noted that the difference between the 700 mb and 500 mb wet bulb potential temperature is a stability index that is essentially the same as if a standard Showalter Index was computed from 850 mb. For those grid points which have terrain heights above 700 mb, no stability index is forecast.

4.3.4 Quantitative Precipitation Forecasts

The technique to calculate a quantitative precipitation forecast (QPF) is similar to the formulation that is reported by Haltiner (1971). This modified formula is

$$Q = \int_{t}^{t+1} \int_{z_l}^{z_u} \frac{dw}{dt} \bar{e} \, dz \, dt \qquad (24)$$

where Q is QPF, w is the saturation mixing ratio of the parcel, and $\bar{e}$ is the standard density for the layer. The integration is over time step, Δt, and over the thickness of a layer $z_u - z_l$. The vertical summation of (24) is done independently at the 500 mb, 700 mb, and 850 mb levels The upper level, z_u, refers to a point midway between the standard pressure level being forecast and the next standard level above it. The same condition is true for z_l, except it is below the forecast level. The amount of precipitation that reaches the surface is the sum of the forecasts for the independent layers.

Generally, the calculation of each of the terms in (24) consists of manipulating quantities that either have been determined or using the methods discussed above. The first variable is the change in the saturation mixing ratio, dw, which is the difference between the mixing ratio at the start and the end of the moist adiabatic expansion. The difference represents the amount of liquid water that condenses and is expressed in units of gm H_2O/kg air. All liquid water is assumed to fall as precipitation. Using equations derived from the definition of the saturation mixing ratio (w_s, w_e), the mixing ratio at the start (subscript s) and at the end (subscript e) of the moist expansion is

$$w_s = 0.622\ (e_s/P_s) \tag{25}$$

$$w_e = 0.622\ (e_e/P_e). \tag{26}$$

The term P_s is the pressure of the LCL and P_e is the standard pressure level for which the forecast is being made.

Saturation vapor pressure (e_s and e_e in the above equations) is calculated in the manner described by Lowe and Ficke (1974). Their technique involves solving a sixth - order polynomial approximation that specifies e as a function of temperature only. The temperatures for this polynomial are those at the beginning and end of the moist expansion. The advantage of using a polynomial solution, rather than one requiring exponentiation, is a faster computation of the variable. As discussed by Lowe and Ficke, accuracy of the approximation is very good.

To this point of the discussion, it has been assumed that total saturation occurs exactly at the LCL. However, condensation and subsequent precipitation have been shown to occur at relative humidity values less than 100 percent when averaged over a large area. To allow for this observation, the terms in (24) are not evaluated at the LCL, but rather at a level below it. It has been determined experimentally at AFGWC that this level is 7 mb below the LCL. This level is identical to a CPS value of 7 mb, and it corresponds to a cloudiness of approximately 95 percent.

The remaining terms in (24), $\overline{e}\,dz$, together represent the weight of air per unit area. When these terms are combined with w, the desired units of weight of water per unit area are obtained. The term, z, is computed using a form of the hydrostatic equation,

$$z = R\ T_e\ \ln\ (P_e/P_u)/g \tag{27}$$

where R is the gas constant and g is the acceleration due to gravity. As reported by Haltiner (1971), the precipitation equation (24) gives good results for synoptic-scale pressure systems in mid-latitudes but it is inadequate in areas of convection, especially in tropical systems.

4.3.5 Cloud Type

Techniques have been developed to combine temperature and CPS in order to classify the types of cloud structures. The primary distinction between cloud types is the distinction between stratiform and cumuliform clouds. A stability value is calculated for the 850 mb, 700 mb, and 500 mb pressure levels to assist in this distinction. This stability determination consists of comparing wet bulb potential temperatures, between two levels. This procedure is identical to the description in Section 4.3.2. For example, if the θ_w at 850 mb is greater than the θ_w at 700 mb, a positive, upward buoyancy exists at the 700 mb level. Should clouds be forecast at a pressure level, positive buoyancy at that level implies cumuliform clouds, whereas negative buoyancy implies stratiform. Vertical cloud structures such as towering cumulus and cumulonimbus are determined by applying these checks at all levels. For example, if the 850 mb level is unstable and forecast clouds exist, the 700 mb cloud and stability are checked. If clouds and upward buoyancy exist at 700 mb, then the 500 mb level is checked. Should upward buoyancy exist at 500 mb, the cloud is typed as a cumulonimbus, but if downward buoyancy exists, the cloud is classified as towering cumulus. Some typical combinations of stability and clouds are shown Figure 12.

4.3.6 Precipitation Type

The primary reason for classifying the types of cloud structures is to provide a basis for determining precipitation type. Forecasts of precipitation types are categorized as either continuous (from stratiform clouds) or showery (associated with cumuliform clouds). The development of criteria to determine precipitation types and their intensities was done by comparing forecast values of cloud type, cloud cover, and static stability to precipitation observations. Results of these comparisons indicate that no precipitation is observed when the total cloud cover is less than 3/8 (37 percent) coverage at a grid point. It should be remembered that values at grid points represent average conditions over a large horizontal area. Therefore, these precipitation forecasts should not be viewed as a point forecast.

For showery precipitation (rainshower, snowshower, and thunderstorm) a cloud type of towering cumulus or cumulonimbus is required. Also, a minimum cloud cover of 25 percent is necessary at either the 850 or 700 mb levels. The distinction between rainshowers and thunderstorms is based primarily upon whether the cloud type is towering cumulus or cumulonimbus. Snow showers occur if the gradient level temperature is less than 273° K.

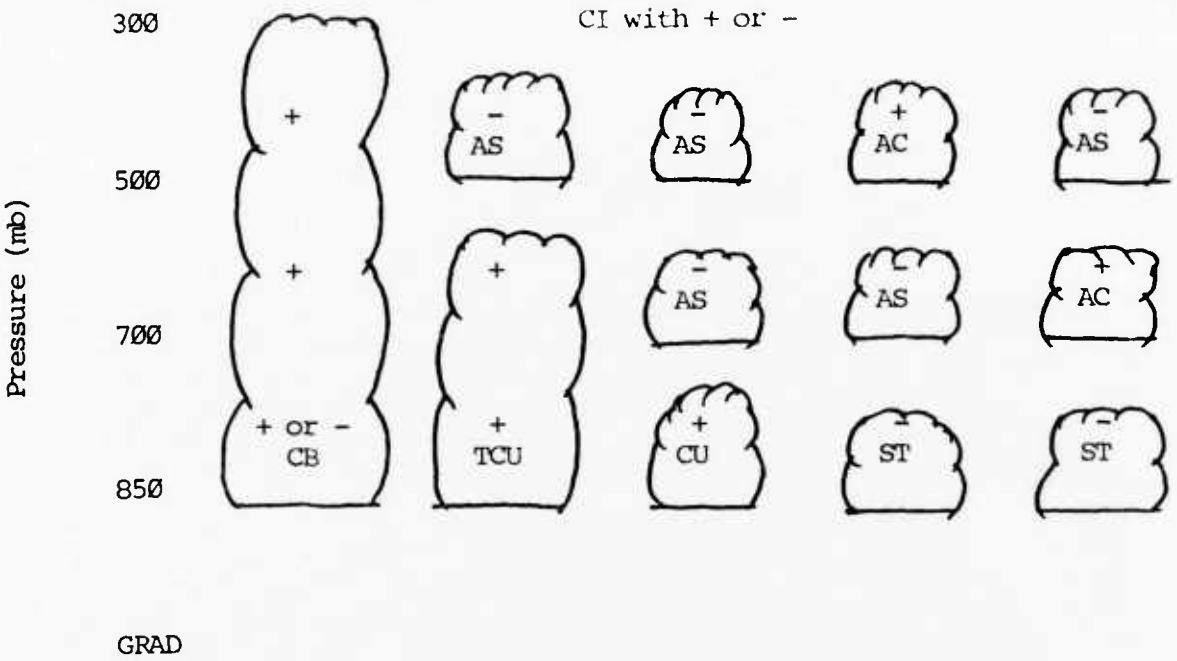

Fig. 12. Some typical cloud types associated with various buoyancies. Buoyancies are determined by the layer difference in wet-bulb potential temperature. Unstable (+) conditions exist if the wet-bulb potential temperature at the lower layer is greater than that at the higher layer. Stable (-) conditions exist if the reverse is true. Due to having information only at discrete layers, it is difficult to make cloud top or base estimates.

The intensity of rainshowers is inferred from the 700 mb static stability, whereas rainshower intensity associated with thunderstorms, is determined by computing a total-totals stability index. This index is defined by Miller (1972). The threshold value differentiating moderate or heavy rainshowers associated with thunderstorms has been correlated with observational evidence. The reader should note that shower-producing mechanisms such as steep terrain and diurnal heating are not considered.

For continuous precipitation (rain, drizzle, and snow) a large areal coverage of cloudiness is required. Cloud types other than towering cumulus or cumulonimbus and cloud cover greater than 75 percent at 850 mb or 700 mb are the minimum criteria for this precipitation type. Snow is differentiated from liquid precipitation whenever the gradient level temperature is less than 273° K.

The intensity for continuous precipitation is a function of the moisture depth and the buoyancy at 700 mb. For example, heavy continuous rain is forecast when cloud amounts are greater than 75 percent at all three levels (850, 700, and 500 mb) and the 850 mb wet-bulb potential temperature is more than 3 K greater than the 700 mb value. Lesser intensities are forecast for shallower cloud depths and smaller buoyancy values.

4.3.7 Icing

Forecasts of icing can be derived using temperature and moisture information. The criteria to forecast icing type and intensity are the same as that in AWS/TR-80/001, Forecaster's Guide on Aircraft Icing. Table 1 is a summary of these criteria. Initially, all icing intensities are light. When cold air advection greater than 2°K/3 hr is forecast, the intensity is increased to moderate. Warm air advection of 0.1°K/3 hr will reduce the intensity to trace. For temperatures outside of the ranges in Table 1, no icing is forecast. All icing intensities are initially classified as light.

Table 1. Icing Forecast Criteria.

TEMPERATURE (K)	DEW POINT DEPRESSION (K)	ICING TYPE	CLOUD TYPE
272-266	-2	Clear	Cumulus
		Rime	Stratus
265-258	-3	Mixed	Cumulus
		Rime	Stratus
257-251	-4	Rime	All Clouds

5. HIGH RESOLUTION CLOUD PROGNOSIS

5.1 Model Specifications

The High-Resolution Cloud Prognosis (HRCP) module forecasts percent cloudiness for 15 levels on an eighth-mesh grid. This eighth-mesh grid coincides with the one used in the RTNEPH (Fig. 13). In addition, a percent total cloudiness is forecast for each eighth-mesh point. Forecasts are made in three-hour time steps to a maximum of 9 hours.

The HRCP is capable of making a forecast for that portion of the eighth-mesh grid within the AFGWC octagon. However, the advection module of the HRCP only forecasts for a single window of this area in any one computer run. This window can be located anywhere in the octagon; however, the window must coincide with one or more of the boxes of the eighth-mesh grid. These boxes are numbered from one to 64 as shown in Fig 13.

5.2 Options

The HRCP can be initiated for any starting hour, and it phases into the 5LAYER database to use the trajectories already stored there. It has the option to make any length forecast out to 9 hours in three-hour increments.

5.3 Forecast Mechanism

The HRCP is initialized directly from the RTNEPH converted to look like the old 3DNEPH database (primarily 15 layers of cloud information). No modification of the cloud amounts is made. To produce an eighth-mesh cloudiness forecast, HRCP uses information available in the 5LAYER and the RTNEPH cloud models. The first major step is to calculate the local change of CPS with time at the half-mesh grid points. Trajectories are available only on the half-mesh grid, the advection of the initial CPS field is done on this grid scale. The local change of CPS results from taking the difference between the initial and forecast CPS fields.

In order to apply this half-mesh, 5LAYER, local tendency of CPS, an eighth-mesh, 15-level format must be used. To do this, the CPS tendency is horizontally interpolated to the eighth-mesh grid points. This tendency is not vertically interpolated, but rather each of the forecast five levels are directly applied to their corresponding levels of the 15-level grid (cloud analysis). For example, the tendency at 300 mb is applied to layers 13, 14, and 15 (Fig. 14).

A slightly different methodology is used for the gradient level. The CPS tendency for this level is applied only to levels five and six. The cloud amounts in levels one to four are persisted. The intent of this method is to eliminate the advection of very low-level clouds. Advection of low clouds such as fog would be a questionable procedure.

Lastly, this CPS tendency is applied directly to the 3DNEPH to produce an eighth-mesh, 15-level cloud forecast. This process is depicted in Fig. 15. In addition, a total cloud forecast is produced by stacking these 15 levels.

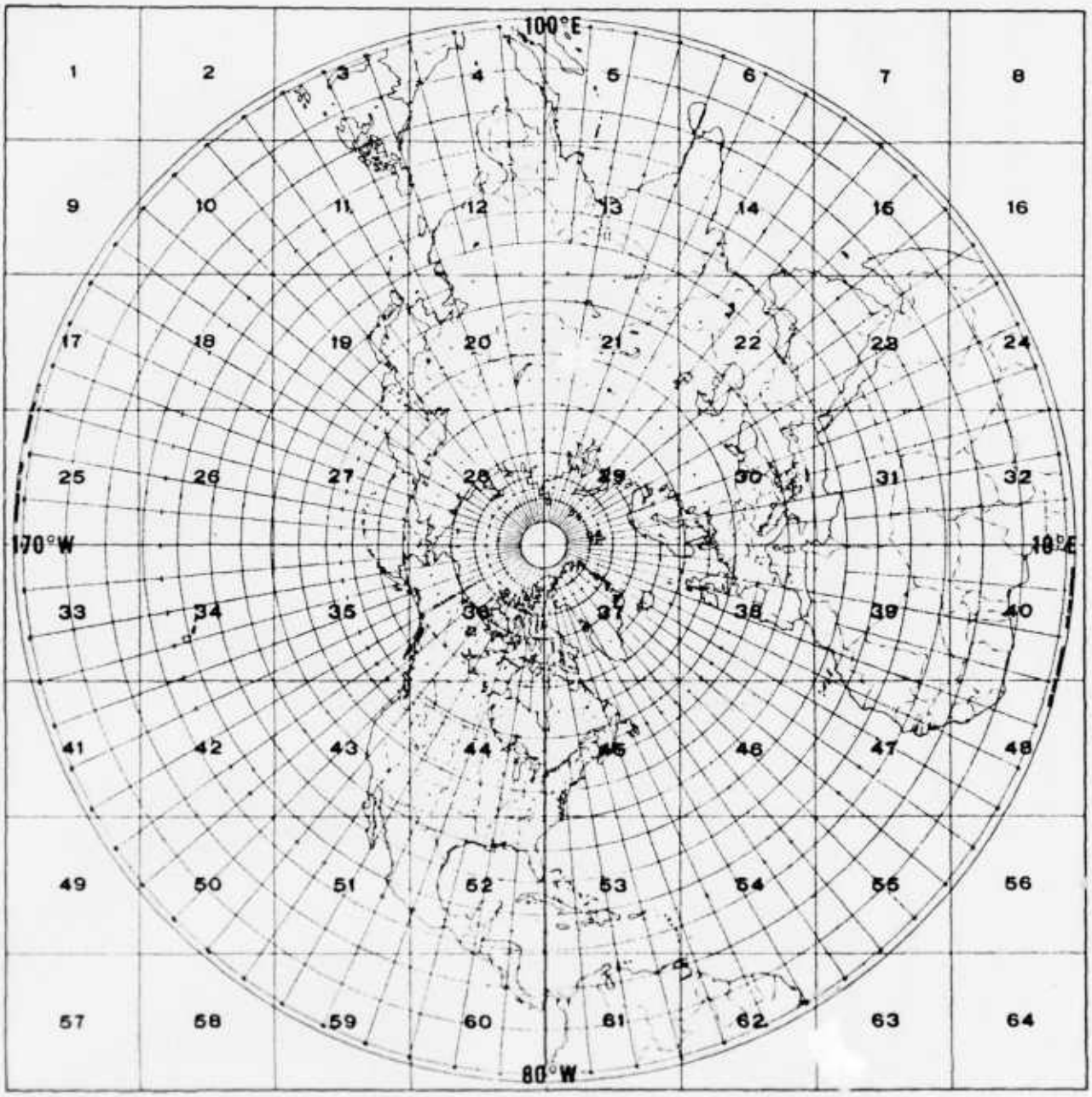

NORTHERN HEMISPHERE

Fig. 13. Northern Hemisphere RTNEPH grid over a polar stereographic projection.

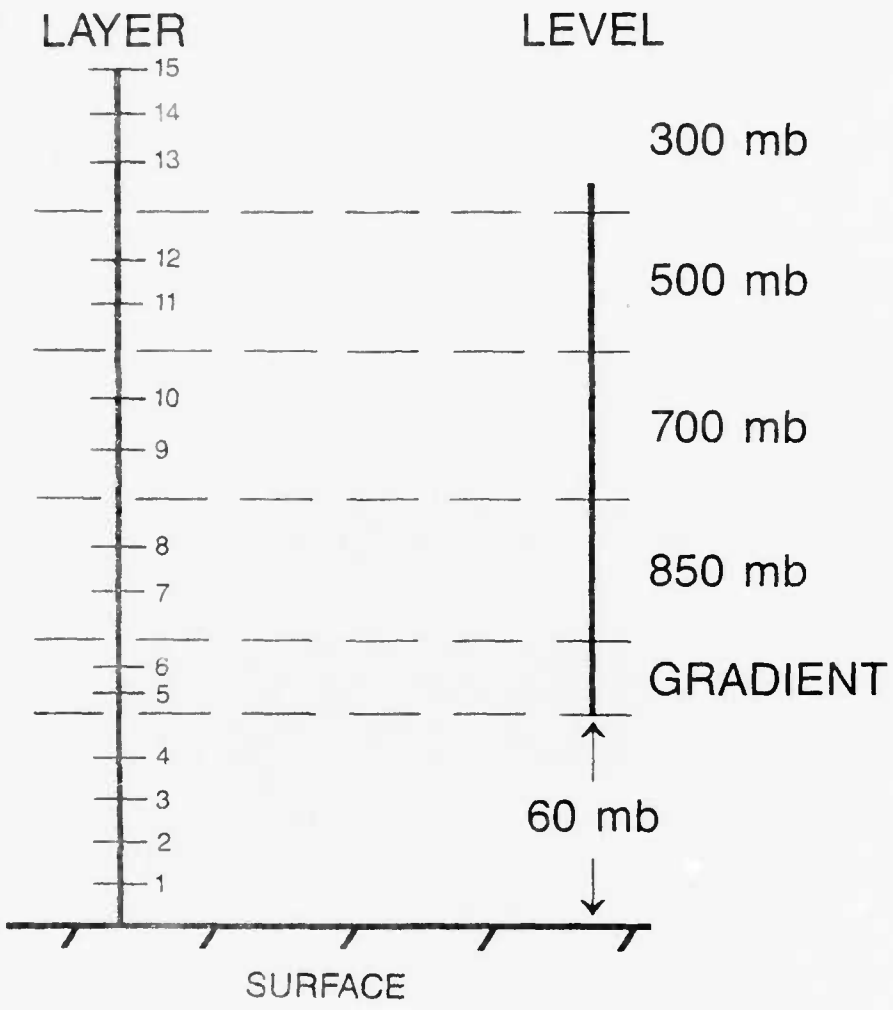

Fig. 14. Association of the 15 fixed levels (left) in HRCP that the trajectories in the five forecast layers of 5LAYER are applied to.

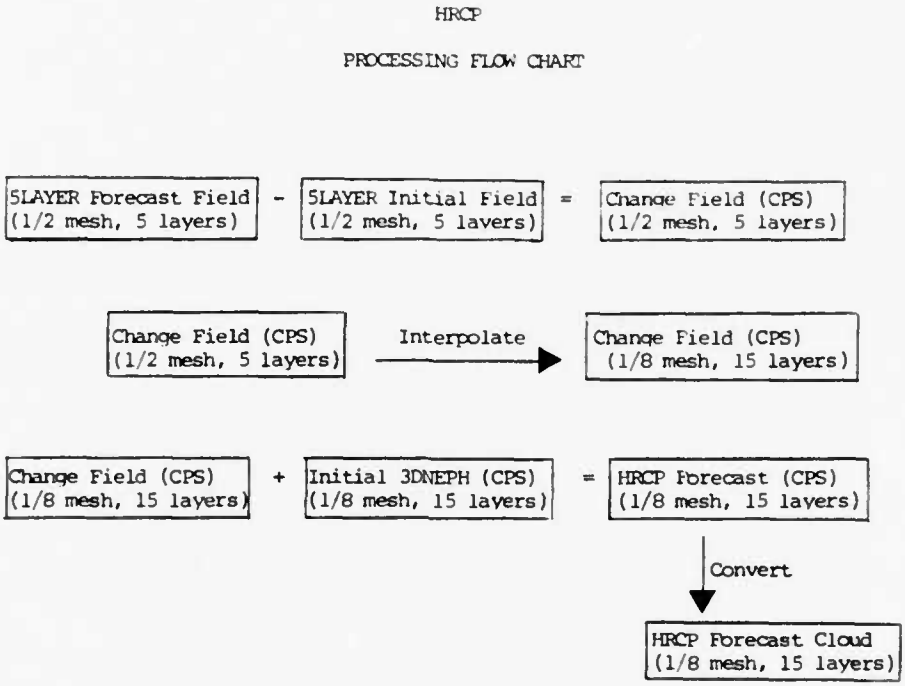

Fig. 15. Flow chart of HRCP processing of 5LAYER and RTNEPH data to produce an eighth-mesh forecast.

6. TROPICAL CLOUD FORECASTS

6.1 Model Specification

The Tropical Cloud Forecasting Model (TRONEW) produces forecasts for three layers (low, middle, and high) on the AFGWC Northern Hemisphere and Southern Hemisphere half-mesh supergrids from approximately 25°N to 25°S. Forecasts are made every three hours in three-hour increments out to 21 hours.

6.2 Forecast Mechanism

TRONEW uses the premise that in the tropics there are diurnal fluctuations of cloudiness; and therefore, clouds that were observed yesterday at a certain time of day will again be observed today at that same time. This premise works well except in the vicinity of moving tropical disturbances (e.g. typhoons, and easterly waves).

To initialize the half-mesh grid, a 9-point weighted average (interior grid points in Fig. 4) of the eighth-mesh RTNEPH grid is used. This compacted analysis is then saved, so that if a six-hour forecast is needed from a 23/0600Z base time, TRONEW will use the 22/1200Z analysis as that forecast.

7. MODEL EVALUATION

7.1 Verification

The primary purpose in verifying any forecast scheme is to provide a basis for future model improvement. Improvement may occur by developing better forecast techniques or by identifying characteristic model strengths and weaknesses. As new techniques are developed and evaluated, they are compared to objective verification statistics. Any model degradation or improvement is immediately identified. Forecasters who use numerical guidance routinely make subjective evaluations of the model output. By identifying situations that typically produce good or bad forecasts, the forecaster can modify the output and therefore improve the forecast.

The 5LAYER model is evaluated by both subjective and objective verification schemes. Forecasters at AFGWC routinely use 5LAYER forecasts to assist them in providing worldwide meteorological support. The Special Support Division and the Forecasting Services Division are the primary users of the 5LAYER model at AFGWC. Special Support forecasters use 5LAYER for their initial forecast guidance and for quality control of the product. Quality control is maintained by comparing verification of the forecaster's product to that of the model.

Forecasting Services Division forecasters use 5LAYER in a similar manner. The Horizontal Weather Depiction (HWD) Section of this division is responsible for forecasting clouds, icing, and precipitation type on a hemispheric coverage. These forecasts provide the primary guidance for similar forecasts that have more specific application. For example, they are used for Strategic Air Command (SAC) low-level route forecasts, Tactical Air Command (TAC) range forecasts, and U.S., European, and Asian terminal forecasts. Because so many forecasts rely on the "lead" forecast of the HWD section, the product is continuously quality controlled.

Objective verification of 5LAYER forecasts is accomplished by automated, model verification programs that produce statistical evaluation of layered and total cloud forecasts. Persistence "forecasts" are also verified as a standard to compare model performance.

Since the RTNEPH is the standard against which cloud forecasts are verified, a discussion of the model's characteristics is necessary. The RTNEPH uses data from all available sources. Satellite, radiosonde reports, standard surface observations, and aircraft reports are merged to produce a hemispheric cloud analysis. Each of these data sources contribute their own characteristics in determining the "true" cloud amount. Satellite data for the RTNEPH is provided by the Defense Meteorological Satellite Program (DMSP). This program normally consists of two polar-orbiting satellites. Sensors on the satellite accurately determine the horizontal cloud coverage. However, the vertical distribution of clouds must be inferred from other data sources. Vertical temperature profiles used with infrared satellite sensors can give approximate vertical positioning. Aircraft reports and surface

observations also aide in this determination. DMSP satellite data, because of polar-type orbits, do not give hourly global coverage. Therefore, at a particular verification time new satellite data may not be available. Since the RTNEPH uses persistence in the absence of new data, a forecast of persistence would verify as being correct.

Most grid points in the model verification program are located over land masses to partially alleviate any bias favorable to the persistence forecast. However, surface observations of clouds contribute their own source of error. The line-of-sight of a surface-based observer is only 10 to 20 miles depending on obstructions and viewing angle with respect to the terrain. These restrictions typically cause surface observers to overestimate horizontal cloud distribution. Low overcast cloud layers bias surface reports by preventing reports of cloud conditions above the overcast. The RTNEPH persists the cloud analysis in the absence of new layered cloud observations. As was discussed for satellites, there continues to be a favorable bias in the verification toward the persistence forecast. Despite these problems the 5LAYER model out performs the persistence forecast. A more complete discussion of the comparative cloud forecast skill of 5LAYER was prepared by Mitchell (1982). Figure 16 provides a graphical representation of the 5LAYER performance during May 1985 to April 1986. The verification variable is the percentage of forecasts of total cloud that verified within $\pm$25% of the total cloud cover analyzed by RTNEPH. As with other forecast models, forecast skill deteriorates with increasing length of forecast.

7.2 Five Layer Model

Numerical models provide an objective means of producing forecasts. When used as a forecaster's aid, they serve as a basis from which a forecaster can produce an improved forecast. By learning inherent characteristics of a model, a forecaster can better manage his use of these aids. Ideally, the forecaster should spend his greatest efforts on situations of known model deficiencies. Conversely, little time should be spent on situations where the model performs well. The purpose of this subsection is to identify strengths and weaknesses of the 5LAYER model.

The 5LAYER model depends on other models to provide cloud and temperature analyses and wind forecasts. Characteristics of these models inherently become a part of the 5LAYER model. Wind forecasts from the AWS GSM model are formed into trajectories as described in Section 3 and Appendix D. Characteristics that are typical of the AWS GSM are also typical of the 5LAYER.

The 5LAYER model produces the best cloud forecasts at mid-tropospheric levels (700 and 500 mb) and at middle latitudes. This should be expected since dynamic wind models (like AWS GSM) produce their best forecasts in his region. Also, clouds that are associated with moderate or strong synoptic-scale weather patterns are identified and forecast with the greatest skill. Again, this is to be expected since mid-latitude storm systems are of a sufficient scale to be resolvable by the 5LAYER grid system. These cloud systems also have well-defined cloud boundaries which are necessary for accurate cloud mapping and for predicting movement of these boundaries.

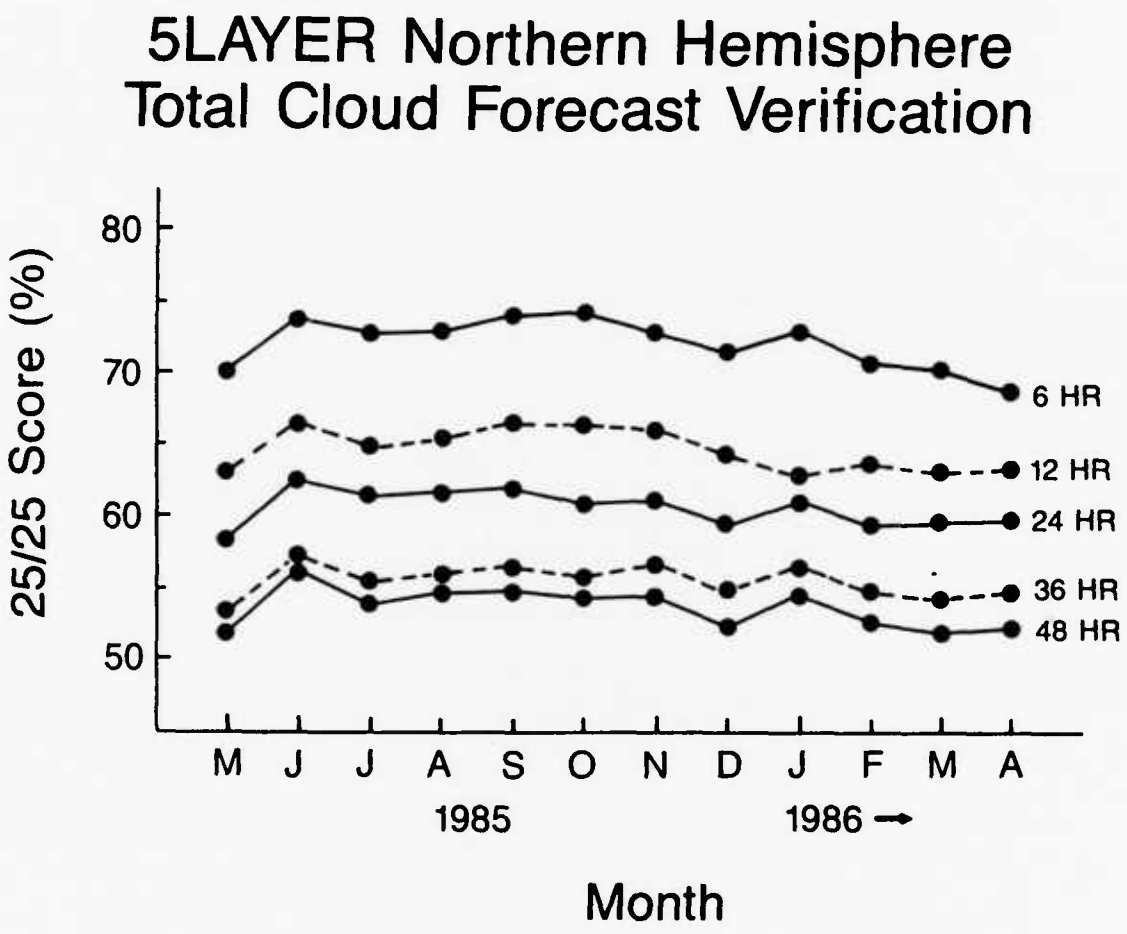

Fig. 16. One year summary of monthly Northern Hemisphere 5LAYER total cloud 25/25 skill scores (percentage of forecasts within ±25% of observed total cloud) for 6, 12, 24, 36, and 48 hour forecasts. Decreasing skill with forecast length is apparent.

RTNEPH data must be put in a workable format for the 5LAYER model. Section 2.2.1 discusses the methodology of locating the vertical the cloud data and representing 25 eighth-mesh grid points by one half-mesh point. Figure 17 shows how horizontal data compaction affects cloud prediction on the larger scale. Figure 17 shows a cloud boundary that is averaged to a half-mesh grid point. Any averaging done across a cloud edge causes a smoothing of that edge. Rather than a distinct change from 100 percent to zero percent cloud cover, the half-mesh representation becomes 100 percent, 50 percent, and zero percent. For large-scale cloud systems, this reduction in cloud mass is not a significant problem. However, for systems represented by only a few grid points, a large percent of the cloud mass may be lost. This loss is solely caused by compacting the cloud data.

Restrictions imposed on the trajectory computation are discussed in Section 3. The effect of these restrictions on cloud prediction has been observed and are discussed here. Trajectories are modified at the lower and lateral boundaries of the 5LAYER grid system. Trajectories near lateral boundaries are restricted to be parallel to the octagon edge. This restriction causes clouds to be advected around the grid edge. This procedure prevents loss of cloud mass from be grid domain. However, clouds are observed to be advected in a direction different than the streamflow.

Trajectories at the lower boundary are also modified to account for terrain effects on cloud formation. As described in Section 3.4, the gradient level trajectories are constrained to follow the terrain surface. Extremely large values of the vertical trajectory component, Δp, are induced by steep terrain features. This effect causes copious amounts of precipitation in regions of steep ascent and very dry conditions in regions of steep descent. This dry bias on the lee side of mountains is advected to other regions. However, it cannot be modified by a moisture source region since no mechanism of this type exists in 5LAYER. To reduce these terrain induced effects, horizontal trajectories are halved if the vertical component exceeds 50 mb/3 hr. A new, reduced vertical component is computed from these shortened trajectories.

Forecasters should be aware that cloud formation and advection near the terrain surface involves complex physical relationships. Parameterizing these relationships produces less than perfect cloud forecasts. However, in the future, advanced computers will explicitly solve these relationships, resulting in improved low-level cloud forecasts.

Cloud and temperature advection is not the only forecast mechanism that effects these parameters. Other sub-scale mechanisms, such as those causing cumulus formation or the surface heating and cooling of temperatures over land masses, are present in the atmosphere. Section 4 describes the parameterization of these and other mechanisms. It should be recognized that in areas where these effects are especially strong, cloud and temperature forecasts from 5LAYER are not explicitly solved. Once additional computer resources are obtained, sub-scale effects on clouds and temperature may be more precisely defined.

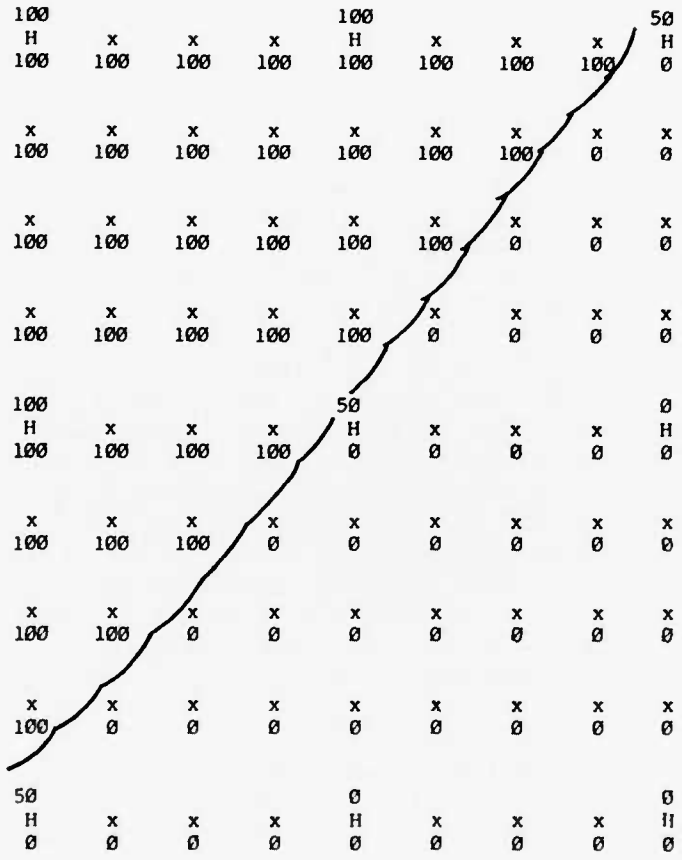

Fig. 17. Depiction of how compaction of eighth-mesh data to half-mesh data eliminates cloud boundary distinction. Eighth-mesh cloud values in percent are below the grid points. Values above the grid points are half-mesh cloud amounts derived from eighth-mesh values.

8. SUMMARY

The cloud forecasting models now in use at AFGWC have evolved over the past 20 years to meet Army, Air Force, and other Department of Defense requirements. Because clouds obstruct visibility, military decision-makers will continue to need cloud forecasts. Increased understanding of the physical processes which cause clouds to form and dissipate as well as increased computer capacity, will provide greater cloud forecasting skill in the future.

The first step in the cloud forecasting model is the initialization of the moisture and temperature values at the grid points. Moisture is derived from the RTNEPH and temperature is obtained from HIRAS. Forecasts are made by advecting the temperature and moisture values with 3-hour Lagrangian trajectories from the AWS GSM model. Before the forecasting can begin, all the variables must be defined at the model grid points by either compacting or interpolating. Currently the cloud data are compacted from 25 nm to 100 nm resolution and the temperature data are interpolated from 200 nm to 100 nm resolution.

Forecasts are made by advecting air parcels along the calculated trajectories. The advected parcel temperature and moisture are modified by vertical displacement, entrainment, evaporation and diurnal effects. The forecast temperature and moisture are used to derive forecasts of dew-point depression, stability, precipitation, cloud type, precipitation type, and icing.

High-resolution cloud forecasts are obtained over limited areas for short forecast periods by interpolating the 100 nm resolution 3-hour moisture changes to 25 nm resolution initial conditions. These forecasts demonstrate a small but significant improvement in skill.

In the tropical regions, forecasts of 24-hour persistence in 3-hour increments have out-performed dynamic models except in areas of moving tropical disturbances.

The compilation of verification statistics for the Five Layer Model and the High Resolution Cloud Prognosis models document the current forecast skill. The movement of synoptic-scale systems depends on the accuracy of the model from which the trajectories are obtained. The parameterizations of entrainment, evaporation, convective development, and diural effects are recognized weaknesses which require the constant attention of the user. The formation and dissipation of low clouds represents another major weakness of the model because these clouds are influenced by terrain features as well as diurnal heating and cooling. A future rewrite of the 5LAYER model will make it global in domain, increase the horizontal resolution, and include better parameterizations to correct the weaknesses stated earlier.

9. REFERENCES

Berry, F. A., E. Bollay and N. R. Beers, 1945: Handbook of Meteorology. McGraw Hill, N. Y., p 343.

Djuric, D., 1961: On the accuracy of air trajectory computerations. J Meteor., 19, 597-605.

Edson, H., 1965: Numerical cloud and icing forecasts. Scientific Services Technical Note 13, 3rd Weather Wing, Air Weather Service (MAC), Offutt AFB NE, 61 pp.

Fye, F. K., 1978: The AFGWC automated cloud analysis model. AFGWC Tech Memo 78-002, AFGWC, Air Weather Service (MAC), Offutt AFB, NE, 97 pp.

Haltiner, G. J., 1971: Numerical Weather Prediction, Wiley, N.Y., p. 317.

Hoke, J. E., J. L. Hayes, and L.G. Renninger, 1985: Map projections and grid systems for meteorological applications. AFGWC/TN-73/003 (REV), AFGWC, Air Weather Service (MAC), Offutt AFB, NE, 87 pp.

Huschke, R. E., 1959: Glossary of Meteorology, American Meteorological Society, Boston, MA, p. 508.

Mitchell, K. E., 1982: Cloud Forecast Fields Comparison Test. AFGWC Technical Note 82/003, AFGWC, Air Weather Services (MAC), Offutt AFB, NE, 65 pp.

Lowe, P. R., and J. M. Ficke, 1974: The computation of saturation vapor pressure. Technical Paper No. 4-74, Environmental Prediction Research Facility, Monterey, CA, 27 pp.

Miller, R. C., 1972: Notes on analysis and severe-storm forecasting procedures at the Air Force Global Weather Central. AWS Technical Report 200 (Rev), Air Weather Service (MAC), Scott AFB, IL, 183 pp.

Reap, R. M., 1971: Air-sea energy exchange in Lagrangian temperature and dew point forecasts. Technical Memorandum NWS TDL-43, NOAA.

Stobie, J. G.., 1986: AFGWC's Advanced Weather Analysis and Prediction System (AWAPS). AWS Technical Note - 86/001, Air Weather Service (MAC), Scott AFB, IL, 68 pp.

Tarbell, T. C., and J. E. Hoke, 1979: The AFGWC automated analysis/forecast model system. AFGWC Technical Note 79-004, AFGWC, Air Weather Service (MAC), Offutt AFB, NE, 52 pp.

Air Weather Service Technical Report 80/001: Forecasters guide on aircraft icing. March 1980, 51 pp (Formerly AWSM 105-39).

10. APPENDIX A. CONDENSATION PRESSURE SPREAD DERIVATION

The derivation of P_s begins by specifying the mixing ratio, w, at any pressure as

$$w = (3.8/P)10^{x} \tag{A1}$$

where

$$x = \frac{a(T_d - 273)}{b + T_d - 273} \tag{A2}$$

This formulation, known as Teten's equation, is found in Berry, Bollay, and Beers (1945). Values of a and b are known constants and depend on whether the process occurs over ice or water. T_d is the dew-point temperature in Kelvin. For the case of saturation w_s is similarly described as

$$w_s = (3.8/P)10^{x_s} \tag{A3}$$

where

$$x_s = \frac{a(T_s - 273)}{b + T_s - 273} \tag{A4}$$

T_s is the condensation temperature in Kelvin. Because of the conservative nature of the dry adiabatic process, the values w and w_s of an air parcel lifted to condensation are unchanged. Therefore

$$(3.8/P)10^{x} = (3.8/P_s)10^{x_s}$$

reordering terms one can write:

$$\log P_s = \log P + (x_s - x). \tag{A5}$$

Using Poisson's equation:

$$T_s = T\,(P_s/P)^{0.286} \tag{A6}$$

and substituting equations (A2), (A4) and (A6) into (A5) the final relationship becomes:

$$\log P_s = \log P + \frac{a[T(\frac{P_s}{P})^{0.286} - 273]}{b[T(\frac{P_s}{P})^{0.286} - 273]} - \frac{a[T_d - 273]}{b + T_d - 273} \tag{A7}$$

While (A7) cannot be directly solved for P_s, if given known values of P, T, T_d, a, and b, one can calculate approximate values of P_s in a recursive fashion. With this approximate value of P_s, the variables in equation (3) are now determined, and the CPS can be calculated.

11. APPENDIX B. TABLES RELATING CONDENSATION PRESSURE SPREAD AND CLOUD AMOUNT

Table B1. Conversion of Cloud Amount to Condensation Pressure Spread

The following four tables are used by 5LAYER to convert from cloud amount in percent to CPS values in mb. Each table is labeled with the pressure level at which it is valid. CPS values are interior to the tables. Units of cloud percent form the abscissa, while tens of cloud percent appear on the ordinate of each table.

Table B1a. 850 mb

	0	1	2	3	4	5	6	7	8	9	10
0	120.0	114.0	111.0	108.2	106.0	103.2	100.5	98.0	95.7	93.7	90.6
10	90.6	88.4	86.0	83.0	81.0	77.7	75.5	73.4	71.0	69.6	68.2
20	68.2	66.8	66.0	64.0	62.6.	61.0	59.6	58.0	56.6	55.8	55.0
30	55.0	53.7	52.5	51.6	50.6	49.0	48.2	47.4	46.6	45.8	45.0
40	45.0	44.2	43.4	42.6	41.8	41.0	40.2	39.4	38.6	37.8	37.0
50	37.0	36.2	35.4	34.8	34.4	34.1	33.7	33.4	33.0	32.6	32.3
60	32.3	31.9	31.6	31.2	30.7	30.3	29.7	29.2	28.8	28.3	27.9
70	27.9	27.5	27.0	26.6	26.1	25.7	25.2	24.7	24.2	23.7	23.2
80	23.2	22.5	21.9	21.2	20.4	19.5	18.6	17.7	16.8	15.6	14.5
90	14.5	13.5	12.4	11.3	10.1	9.0	7.6	6.0	4.2	2.6	1.0

Table B1b. 700 mb

	0	1	2	3	4	5	6	7	8	9	10
0	109.0	107.0	105.0	102.8	100.8	99.2	96.7	95.6	94.5	93.4	92.2
10	92.2	91.0	90.2	89.4	87.0	86.0	85.0	83.2	81.0	79.0	77.0
20	77.0	75.2	73.3	71.5	70.0	68.3	66.9	65.3	63.9	62.4	61.0
30	61.0	59.8	58.7	57.5	56.2	55.1	54.0	52.9	51.8	50.7	49.8
40	49.8	48.8	48.0	47.1	46.2	45.3	44.5	43.7	42.8	41.9	41.0
50	41.0	40.7	40.3	40.0	39.6	39.3	38.9	38.6	38.2	37.9	37.6
60	37.6	37.2	36.8	36.4	36.0	35.6	35.2	34.8	34.3	33.6	33.3
70	33.3	32.8	32.2	31.8	31.3	30.7	30.2	29.6	29.0	28.4	27.9
80	27.9	27.3	26.7	26.2	25.6	25.0	24.2	23.4	22.4	21.4	20.0
90	20.0	18.4	17.3	16.0	14.5	13.2	11.4	9.6	7.2	4.7	1.0

Table B1c. 500 mb

	0	1	2	3	4	5	6	7	8	9	10
0	101.0	100.2	99.4	98.6	97.8	97.1	96.2	95.4	94.5	93.7	92.9
10	92.9	92.1	91.4	90.6	89.8	89.0	88.0	87.0	85.0	83.0	81.0
20	81.0	79.3	77.7	76.0	74.3	72.7	71.0	70.2	69.3	68.4	67.5
30	67.5	66.7	65.8	64.9	64.0	63.2	62.3	61.5	60.0	58.3	56.4
40	56.4	54.7	52.0	51.0	50.3	49.6	48.9	48.3	47.6	46.9	46.1
50	46.1	45.5	44.8	44.1	43.4	42.7	42.0	41.3	40.8	40.4	40.0
60	40.0	39.6	39.2	38.8	38.4	38.0	37.6	37.2	36.8	36.3	35.9
70	35.9	35.5	35.0	34.6	34.2	33.7	33.3	32.8	32.1	31.5	30.7
80	30.7	29.7	28.8	28.0	27.2	26.2	25.1	24.0	23.0	21.9	20.7
90	20.7	19.6	18.3	16.9	15.3	13.4	11.4	9.4	7.4	5.0	1.0

Table B1d. 300 mb

	0	1	2	3	4	5	6	7	8	9	10
0	97.0	96.2	95.4	94.6	93.8	93.2	92.2	91.4	90.5	89.7	88.9
10	88.9	88.1	87.4	86.6	85.8	85.0	84.5	84.0	83.5	83.0	81.0
20	81.0	79.3	77.7	76.0	74.3	72.7	71.0	70.2	69.3	68.4	67.5
30	67.5	66.7	65.8	64.9	64.0	63.2	62.3	61.5	60.0	58.3	56.4
40	56.4	54.7	52.0	51.0	50.3	49.6	48.9	48.3	47.6	46.9	46.1
50	46.1	45.5	44.8	44.1	43.4	42.7	42.0	41.3	40.8	40.4	40.0
60	40.0	39.6	39.2	38.8	38.4	38.0	37.6	37.2	36.8	36.3	35.9
70	35.9	35.5	35.0	34.6	34.2	33.7	33.3	32.8	32.1	31.5	30.7
80	30.7	29.7	28.8	28.0	27.2	26.2	25.1	24.0	23.0	21.9	20.7
90	20.7	19.6	18.3	16.9	15.3	13.4	11.4	9.4	7.4	5.0	1.0

Table B2. Conversion of Condensation Pressure Spread to Percent of Cloud

The following four tables are used by 5LAYER to convert from CPS in mb to cloud amount in percent. Each table is labeled with the pressure level at which it is valid. Cloud values are interior to the tables. Units of CPS form the abscissa, while tens of CPS appear on the ordinate of each table.

Table B2a. 850 mb

	0	1	2	3	4	5	6	7	8	9	10
0	100.0	100.0	99.4	98.7	98.1	97.6	97.0	96.4	95.7	95.0	94.1
10	94.1	93.3	92.4	91.5	90.5	89.5	88.7	87.8	86.7	85.5	84.4
20	84.4	83.3	81.8	80.3	78.4	76.4	74.3	72.1	69.8	67.5	65.5
30	65.5	63.5	60.8	58.0	55.2	52.5	51.2	50.0	48.7	47.5	46.2
40	46.2	45.0	43.7	42.5	41.2	40.0	38.7	37.5	36.2	35.0	34.3
50	34.3	33.7	32.6	31.5	30.8	30.0	28.7	27.5	27.0	26.5	25.7
60	25.7	25.0	24.4	23.7	23.0	22.2	22.0	20.8	20.1	19.5	18.7
70	18.7	18.0	17.6	17.2	16.7	16.2	15.8	15.3	14.9	14.5	14.2
80	14.2	14.0	13.5	13.0	12.7	12.5	12.0	11.6	11.2	10.7	10.3
90	10.3	9.8	9.6	9.4	8.8	8.2	7.9	7.5	7.0	6.6	6.2
100	6.2	5.8	5.4	5.1	4.7	4.4	4.0	3.6	3.1	2.7	2.3
110	2.3	2.0	1.6	1.2	1.0	.8	.7	.5	.4	.2	.0

Table B2b. 700 mb

	0	1	2	3	4	5	6	7	8	9	10
0	100.0	100.0	99.9	99.7	99.3	98.9	98.5	98.1	97.7	97.3	96.8
10	96.8	96.2	95.7	95.2	94.4	93.6	93.0	92.3	91.4	90.5	90.0
20	90.0	89.4	88.4	87.5	86.2	85.0	83.3	81.5	79.8	78.0	76.3
30	76.3	74.5	72.5	70.5	68.5	66.5	64.0	61.6	58.7	55.8	52.9
40	52.9	50.0	48.9	47.8	46.6	45.3	44.2	43.1	42.0	40.8	39.8
50	39.8	38.7	37.8	36.9	36.0	35.1	34.2	33.4	32.6	31.7	30.8
60	30.8	30.0	29.3	28.6	27.9	27.2	26.6	25.9	25.2	24.6	24.0
70	24.0	23.3	22.7	22.2	21.6	21.1	20.5	20.0	19.5	19.0	18.5
80	18.5	18.0	17.6	17.1	16.6	16.0	15.0	14.0	13.8	13.5	12.2
90	12.2	11.0	10.2	9.4	8.5	7.5	6.6	5.8	5.4	5.1	4.5
100	4.5	3.9	3.4	2.9	2.5	2.0	1.5	1.0	.5	.0	.0
110	.0	.0	.0	.0	.0	.0	.0	.0	.0	.0	.0

Table B2c. 500 mb

	0	1	2	3	4	5	6	7	8	9	10
0	100.0	100.0	99.8	99.5	99.3	99.0	98.6	98.2	97.7	97.2	96.7
10	96.7	96.2	95.7	95.2	94.7	94.2	93.6	92.9	92.2	91.5	90.6
20	90.6	89.8	88.9	88.0	87.0	86.1	85.2	84.2	83.0	81.7	80.7
30	80.7	79.7	78.2	76.7	74.4	72.1	69.8	67.5	65.0	62.5	60.0
40	60.0	57.5	56.0	54.6	53.2	51.7	50.2	48.8	47.4	45.9	44.5
50	44.5	43.0	42.0	41.9	41.4	40.8	40.2	39.7	39.2	38.6	38.0
60	38.0	37.5	36.4	35.2	34.0	32.9	31.8	30.6	29.4	28.3	27.2
70	27.2	26.0	25.4	24.8	24.2	23.6	23.0	22.4	21.8	21.2	20.6
80	20.6	20.0	19.5	19.0	18.5	18.0	17.5	17.0	16.0	15.0	13.8
90	13.8	12.5	11.2	9.8	8.6	7.5	6.3	5.1	3.8	2.5	1.2
100	1.2	.0	.0	.0	.0	.0	.0	.0	.0	.0	.0
110	.0	.0	.0	.0	.0	.0	.0	.0	.0	.0	.0

Table B2d. 300 mb

	0	1	2	3	4	5	6	7	8	9	10
0	100.0	100.0	99.8	99.5	99.3	99.0	98.6	98.2	97.7	97.2	96.7
10	96.7	96.2	95.7	95.2	94.7	94.2	93.6	92.9	92.2	91.5	90.6
20	90.6	89.8	88.9	88.0	87.0	86.1	85.2	84.2	83.0	81.7	80.7
30	80.7	79.7	78.2	76.7	74.4	72.1	69.8	67.5	65.0	62.5	60.0
40	60.0	57.5	56.0	54.6	53.2	51.7	50.2	48.8	47.4	45.9	44.5
50	44.5	43.0	42.0	41.9	41.4	40.8	40.2	39.7	39.2	38.6	38.0
60	38.0	37.5	36.4	35.2	34.0	32.9	31.8	30.6	29.4	28.3	27.2
70	27.2	26.0	25.4	24.8	24.2	23.6	23.0	22.4	21.8	21.2	20.6
80	20.6	20.0	19.5	19.0	17.0	15.0	13.8	12.5	11.2	9.8	8.6
90	8.6	7.5	6.3	5.1	3.8	2.5	1.2	.0	.0	.0	.0
100	.0	.0	.0	.0	.0	.0	.0	.0	.0	.0	.0
110	.0	.0	.0	.0	.0	.0	.0	.0	.0	.0	.0

12. APPENDIX C WHOLE-MESH TO HALF MESH INTERPOLATION

The interpolation method developed to initialize 5LAYER half-mesh fields from whole-mesh fields is one where successive passes are made on the half-mesh octagon. Each pass uses results of previous passes to interpolate different sets of points. The passes are as follows:

Note: <wgt> denotes the point weight
# denotes a whole-mesh point
+ denotes a previously interpolated half-mesh point
● denotes point being interpolated

Pass #0: Unpacks the whole-mesh data, multiplies each point by 48 (to prevent round-off errors with integer arithmetic), and assigns them to the appropriate half-mesh point. This pass is performed once to prepare the data for interpolation.

Pass #1: Interpolate the diagonal octagon boundary points.

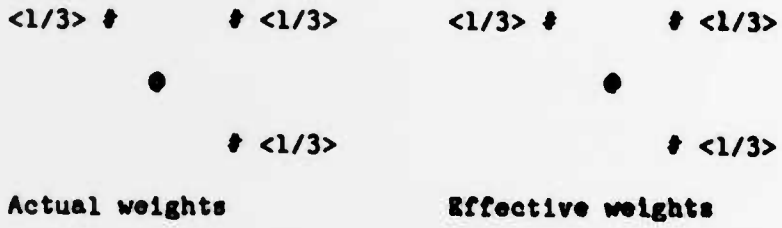

Pass #2: Interpolate the octagon interior, using only whole mesh equivalent points.

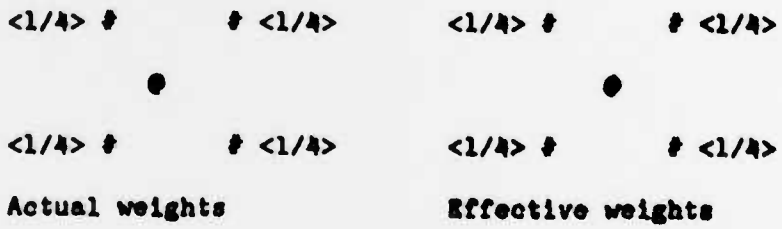

Pass #3: Interpolate remaining octagon boundary points using results from Pass #2.

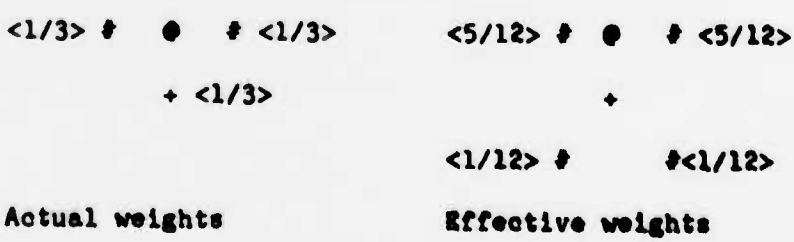

Pass #4: Interpolate along constant J (rows), between whole-mesh equivalent points, using results from Passes #1 and #2.

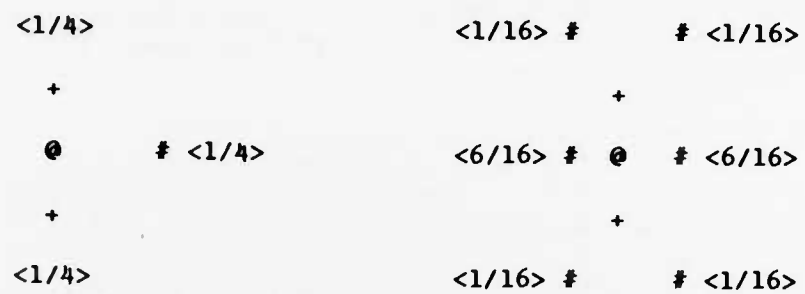

Actual weights Effective weights

Pass #5: Interpolate along constant I (columns), between whole-mesh equivalent points, using results from Passes #1 and #2.

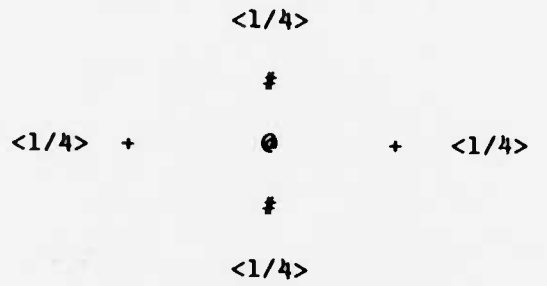

Actual weights

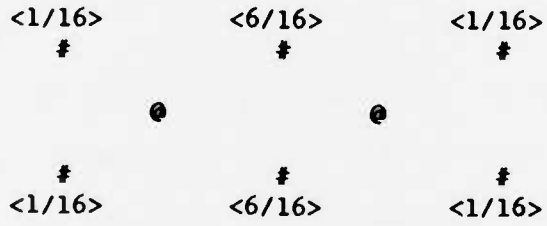

Effective weights

Pass #6: Divide each half-mesh point by 48, and pack into the appropriate half-mesh data array.

13. APPENDIX D. COMPUTATION OF TRAJECTORIES.

A derivation of the equations that are used to compute the trajectory displacements (Section 3) in the 5LAYER cloud model follows.

Given an air parcel which follows a three-dimensional trajectory in its motion from a starting point S to end point E, we want to express the upstream displacement from point E to point S in an x, y, p coordinate system in terms of the mean wind components u, v, and ω valid over the time interval, Δt, of the parcel's motion:

$$\Delta x = -\bar{u}\Delta t$$

$$\Delta y = -\bar{v}\Delta t \qquad \text{(D1)}$$

$$\Delta p = -\bar{\omega}\Delta t$$

Let u_e, v_e, and ω_e be equal to wind components at the trajectory end point averaged over the time interval, Δt, and u_s, v_s, and ω_s be equal to wind components at the trajectory starting point averaged over the time interval Δt:

The wind components u_s, v_s, and ω_s can be expressed in terms of a Taylor series expansion in the three coordinate directions about the point E where the terms containing partial derivatives higher than first order have been truncated:

$$u_s = u_e + \frac{\partial u}{\partial x}\Delta x + \frac{\partial u}{\partial y}\Delta y + \frac{\partial u}{\partial P}\Delta P$$

$$v_s = v_e + \frac{\partial v}{\partial x}\Delta x + \frac{\partial v}{\partial y}\Delta y + \frac{\partial v}{\partial P}\Delta P \qquad \text{(D2)}$$

$$\omega_s = \omega_e + \frac{\partial \omega}{\partial x}\Delta x + \frac{\partial \omega}{\partial y}\Delta y + \frac{\partial \omega}{\partial P}\Delta P$$

The partial derivatives in equations (D2) are of the wind components averaged over the time interval Δt.

By assuming

$$\bar{u} = 1/2(u_e + u_s)$$

$$\bar{v} = 1/2(v_e + u_s) \qquad \text{(D3)}$$

$$\bar{\omega} = 1/2(\omega_e + \omega_s)$$

and substituting the expressions in (D2) for u_s, v_s, and ω_s, we get

$$\bar{u} = u_e + \frac{1}{2}\frac{\partial u}{\partial x}\Delta x + \frac{1}{2}\frac{\partial u}{\partial y}\Delta y + \frac{1}{2}\frac{\partial u}{\partial P}\Delta P$$

$$\bar{v} = v_e + \frac{1}{2}\frac{\partial v}{\partial x}\Delta x + \frac{1}{2}\frac{\partial v}{\partial y}\Delta y + \frac{1}{2}\frac{\partial v}{\partial P}\Delta P \qquad \text{(D4)}$$

$$\bar{\omega} = \omega_e + \frac{1}{2}\frac{\partial \omega}{\partial x}\Delta x + \frac{1}{2}\frac{\partial \omega}{\partial y}\Delta y + \frac{1}{2}\frac{\partial \omega}{\partial P}\Delta P$$

Equations (D4) can be written as follows by substituting for Δx, Δy, and Δp from equations (D1):

$$\bar{u} = u_e - \frac{1}{2}\frac{\partial u}{\partial x}\Delta t\bar{u} - \frac{1}{2}\frac{\partial u}{\partial y}\Delta t\bar{v} - \frac{1}{2}\frac{\partial u}{\partial P}\Delta t\bar{\omega}$$

$$\bar{v} = v_e - \frac{1}{2}\frac{\partial v}{\partial x}\Delta t\bar{u} - \frac{1}{2}\frac{\partial v}{\partial y}\Delta t\bar{v} - \frac{1}{2}\frac{\partial v}{\partial P}\Delta t\bar{\omega} \qquad \text{(D5)}$$

$$\bar{\omega} = \omega_e - \frac{1}{2}\frac{\partial \omega}{\partial x}\Delta t\bar{u} - \frac{1}{2}\frac{\partial \omega}{\partial y}\Delta t\bar{v} - \frac{1}{2}\frac{\partial \omega}{\partial P}\Delta t\bar{\omega}$$

Equations (D5) form a system of three equations in three unknowns, u, v, and ω, which can be written in matrix form as

$$\begin{bmatrix} 1 + \frac{1}{2}\frac{\partial u}{\partial x}\Delta t & \frac{1}{2}\frac{\partial u}{\partial y}\Delta t & \frac{1}{2}\frac{\partial u}{\partial P}\Delta t \\ 1 + \frac{1}{2}\frac{\partial v}{\partial x}\Delta t & \frac{1}{2}\frac{\partial v}{\partial y}\Delta t & \frac{1}{2}\frac{\partial v}{\partial P}\Delta t \\ 1 + \frac{1}{2}\frac{\partial \omega}{\partial x}\Delta t & \frac{1}{2}\frac{\partial \omega}{\partial y}\Delta t & \frac{1}{2}\frac{\partial \omega}{\partial P}\Delta t \end{bmatrix} \begin{bmatrix} \bar{u} \\ \bar{v} \\ \bar{\omega} \end{bmatrix} = \begin{bmatrix} u_e \\ v_e \\ \omega_e \end{bmatrix} \qquad \text{(D6)}$$

The matrix equation AX = B, has a nontrivial solution vector X, provided $|A| \neq 0$.

To get (D6) in a simplified form, we let

$$e_x = 1 + \frac{1}{2}\frac{\partial u}{\partial x}\Delta t \quad a_y = \frac{1}{2}\frac{\partial u}{\partial y}\Delta t \quad a_p = \frac{1}{2}\frac{\partial u}{\partial P}\Delta t$$

$$b_x = 1 + \frac{1}{2}\frac{\partial v}{\partial x}\Delta t \quad e_y = \frac{1}{2}\frac{\partial v}{\partial y}\Delta t \quad b_p = \frac{1}{2}\frac{\partial v}{\partial P}\Delta t \qquad \text{(D7)}$$

$$c_x = 1 + \frac{1}{2}\frac{\partial \omega}{\partial x}\Delta t \quad c_y = \frac{1}{2}\frac{\partial \omega}{\partial y}\Delta t \quad e_p = \frac{1}{2}\frac{\partial \omega}{\partial P}\Delta t$$

to get:

$$\begin{bmatrix} e_x & a_y & a_p \\ b_x & e_y & b_p \\ c_x & c_y & e_p \end{bmatrix} \qquad \begin{bmatrix} \bar{u} \\ \bar{v} \\ \bar{\omega} \end{bmatrix} \qquad = \qquad \begin{bmatrix} u_e \\ v_e \\ \omega_e \end{bmatrix} \tag{D8}$$

$$A \qquad\qquad X \qquad\qquad B$$

By Cramer's rule,

$$\bar{u} = \frac{|A_1|}{|A|} \qquad\qquad \bar{\omega} = \frac{|A_3|}{|A|}$$

$$\bar{v} = \frac{|A_2|}{|A|} \tag{D9}$$

where

$$|A_1| = \begin{vmatrix} u_e & a_y & a_p \\ v_e & e_y & b_p \\ \omega_e & c_y & e_p \end{vmatrix}$$

$$|A_2| = \begin{vmatrix} e_x & u_e & a_p \\ b_x & v_e & b_p \\ c_x & \omega_e & e_p \end{vmatrix} \qquad |A_3| = \begin{vmatrix} e_x & a_y & u_e \\ b_x & e_y & v_e \\ c_x & c_y & \omega_e \end{vmatrix} \tag{D10}$$

Expanding the expressions for D1, D2, D3, and A we get

$$
\begin{aligned}
|A_1| &= u_e(e_y e_p - c_y b_p) - a_y(v_e e_p - \omega_e b_p) + a_p(v_e c_y - \omega_e e_y) \\
|A_2| &= e_x(v_e e_p - \omega_e b_p) - u_e(b_x e_p - b_p c_x) + a_p(b_x \omega_e - c_x v_e) \\
|A_3| &= e_x(e_y \omega_e - c_y v_e) - a_y(b_x \omega_e - c_x v_e) + u_e(b_x c_y - c_x e_y) \\
|A| &= e_x(e_y e_p - c_y b_p) - a_y(b_x e_p - c_x b_p) + a_p(b_x c_y - c_x e_y).
\end{aligned}
\tag{D11}
$$

Each of the terms in parentheses in equations (D11) appears more than once, hence, to simplify equations (D11), let

$$
\begin{aligned}
&c_1 = (e_y\, e_p - c_y\, b_p), \quad c_2 = (b_x\, e_p - c_x\, b_p), \\
&c_3 = (b_x\, c_y - c_x\, e_y), \quad d_1 = (v_e\, e_p - \omega_e\, b_p) \\
&d_2 = (v_e\, c_y - \omega_e\, e_y), \quad d_3 = (b_x\, \omega_e - c_x\, v_e).
\end{aligned}
\tag{D12}
$$

Equations (D11) then become

$$
\begin{aligned}
|A_1| &= u_e\, c_1 - a_y\, d_1 + a_p\, d_2, \\
|A_2| &= e_x\, d_1 - u_e\, c_2 + a_p\, d_3, \\
|A_3| &= -e_x\, d_2 - a_y\, d_3 + u_e\, c_3, \\
|A| &= e_x\, c_1 - a_y\, c_2 + a_p\, c_3.
\end{aligned}
\tag{D13}
$$

Substituting from equations (D13) into equations (D9), we get

$$\bar{u} = \frac{u_e c_1 - a_y d_1 + a_p d_2}{e_x c_1 - a_y c_2 + a_p c_3}$$

$$\bar{v} = \frac{e_x d_1 - u_e c_2 + a_p d_3}{e_x c_1 - a_y c_2 + a_p c_3} \qquad \text{(D14)}$$

$$\bar{\omega} = \frac{-e_x d_2 - a_y d_3 + u_e c_3}{e_x c_1 - a_y c_2 + a_p c_3}$$

Equations (D7), (D12), and (D14) together yield explicit solutions for $\bar{u}$, $\bar{v}$, and $\bar{\omega}$ which are then used in equations (D1) to compute the upstream displacements from point e, a grid point, to point s.

Using the forecast wind computed by a coarse-mesh wind model, trajectories are computed explicitly at all coarse-mesh grid points on the AFGWC octagon excluding the points on the boundaries. The goal is to interpolate trajectory components from the coarse mesh to the intervening half-mesh grid points. However, before doing this, the trajectories computed explicitly in the vicinity of the boundaries must be checked and modified, if necessary, to ensure that they do not originate outside the octagon. (The coarse-mesh trajectories on the boundaries are derived using the trajectories at grid points indented one coarse-mesh grid unit once the check is accomplished.)

A zone indented two coarse-mesh grid units from the octagon boundary is chosen in which the trajectories are to be constrained to permit flow only toward or parallel to the boundaries. This is easily done for the rows and columns of grid points parallel to the x and y coordinate axes. The grid points parallel to the diagonal boundaries are constrained using vector operations which are described below. The local unit vector perpendicular to each of the diagonal boundaries is defined as

$$\vec{u} = \pm 0.7071\,\vec{i} \pm 0.7071\,\vec{j} \tag{D15}$$

where $\vec{i}$ and $\vec{j}$ are unit vectors parallel to the x and y coordinate axes respectively. The horizontal component of a three dimensional trajectory defined by the vector

$$\vec{D} = \Delta x\vec{i} + \Delta y\vec{j} \tag{D16}$$

is examined to see if it has a component along $\vec{u}$ directed inward. Let θ be the angle between $\vec{u}$ and $\vec{D}$. By definition,

$$\cos\theta = \frac{\vec{u} \cdot \vec{D}}{|\vec{u}|\ |\vec{D}|} \tag{D17}$$

Consequently, if the vector dot product of $\vec{u}$ and $\vec{D}$ is not zero, then $\cos\theta$ is not zero, and $\vec{D}$ has a component along $\vec{u}$ directed toward the interior of the grid. This component is defined by the vector

$$\vec{P} = \frac{\vec{u} \cdot \vec{D}}{\vec{u} \cdot \vec{u}}\,\vec{u} \tag{D18}$$

The component of $\vec{D}$ parallel to the diagonal boundary is defined by

$$\vec{M} = \vec{D} - \vec{P} \tag{D19}$$

The horizontal components of the three-dimensional trajectory are then set equal to those of $\vec{M}$. If $\cos\theta = 0$, then the trajectory is not adjusted.

With the above adjustments accomplished, the trajectories at coarse-mesh grid points on the octagon boundaries parallel to the x and y axes are set equal to the trajectories at grid points indented one coarse-mesh row. Trajectories at coarse-mesh grid points on the diagonal boundaries are computed by averaging the trajectory components at the two closest indented coarse-mesh grid points.

After the preceeding method is accomplished, trajectories are available at all coarse-mesh grid points. These trajectories are then interpolated to all of the intervening half-mesh grid points of the AFGWC octagon.

DISTRIBUTION

AWS/DN, Scott AFB, IL 62225-5008.....3
AWS/DO, Scott AFB, IL 62225-5008.....1
AWS/SY, Scott AFB, IL 62225-5008.....1
OL-A, HQ AWS, Buckley ANG Base, Aurora, CO 8001-9599.....1
AFOTEC/WE, KIRTLAND AFB, NM 87117-7001.....1
SD/YDA, PO Box 92960, Worldway Postal Ctr, Los Angeles, CA 90009-2960.....1
OL-G, HQ AWS, NHC Rm 631, 1320 S Dixie Hwy, Coral Gables, FL 33146-2976.....1
OL-H, HQ AWS, (ATSI-CD-CS-SWO), Ft Huachuca, AZ 85613-7000.....1
OL-L, HQ AWS, Keesler AFB, MS 39534-5000.....1
DET 1, HQ AWS, Pentagon, Washington, DC 20330-6560.....1
DET 2, HQ AWS, Pentagon, Washington, DC 20330-6560.....1
AFSCF/WE, PO Box 3430, Sunnyvale AFS, CA 94088-3430.....1
DET 8, HQ AWS, PO Box 4239N, Las Vegas, NV 89030.....1
DET 9, HQ AWS, PO Box 12297, Las Vegas, NV 89112-0297.....1
1WW/DN, Hickman AFB HI 96853-5000.....3
20WS/DON,APO San Francisco 96328-5000.....1
30WS/DON,APO San Francisco 96301-0420.....1
2WW/DN, APO New York 09012-5000.....3
7WS/DON, APO New York 09403-5000.....1
28WS/DON, APO New York 09127-5000.....1
31WS/DON, APO New York 09223-5000.....1
3WW/DN, Offutt AFB NE 68113-5000.....3
9WS/DON, March AFB, CA 92518-5000.....1
11WS/DON, Elmendorf AFB, AK 99506-5000.....1
24WS/DON, Randolph AFB, TX 78150-5000.....1
26WS/DON, Barksdale AFB, LA 71110-5002.....1
4WW/DN, Peterson AFB, CO 80914-5000.....3
2WS/DON, Andrews AFB, MD 20331-5000.....1
5WW/DN, Langley AFB, VA 23665-5000.....3
1WS/DON, MacDill AFB, FL 33608-5000.....1
3WS/DON, Shaw AFB, SC 29152-5000.....1
5WS/DON, Ft McPherson, GA 30330-5000.....1
25WS/DON, Bergstrom AFB, TX 78743-5000.....1
AFGWC/SDSL, Offutt AFB, NE 68113-5000.....40
USAFETAC/LDO, Scott AFB, IL 62225-5438.....5
AFGWC OL-A, Monterey, CA 93943-5105.....1
AFGWC OL-C, NOAA/NESDIS, E/SPI, MailStop E, Federal BLdg 4,.....1
Washington, DC 20233-0001.....1
7WW/DN, Scott AFB, IL 62225-5008.....3
6WS, Hurlburt Field, FL 32544-5000.....1
15WS/DON, McGuire AFB, NJ 08641-5002.....1
17WS/DON, Travis AFB, CA 94535-50000.....1
3350 TCHTG/TTGU-W, Stop 62, Chanute AFG, 61868-5000.....3
Naval Research Laboratory, Code 4323, Washington, DC 20375.....1
NAVOCEANCOMFAC, NSTL, Bay St Louis, MS 39529-5002.....1

NOCD, Offutt AFB, NE, 68113-5000.....1
COMNAVOCEAN, NSTL, MS 39529-5000.....1
NEPRF, Monterey, CA 93943-5106.....1
FNOC, Monterey, CA, 93943-51005.....1
AFGL Library, Attn: SULLR, Stop 29, Hanscon AFB, MA 01731-5000.....3
AFGL/LY, Hanscom AFB, MA 01731-5000.....5
Atmospheric Sciences Laboratory, White Sands Missile Range, NM 88002-5501.....1
Technical Library, Dugway Proving Ground Dugway, UT 84033-5501.....1
AWSTL, Scott AFB, IL 62225-5438.....5
NOAA (W/FC), Federal Coordinators Office, Rockville, MD 20852.....1
National Meteorological Center, NOAA/W1NMC, Washington DC 20033.....1